Published Ahead of Print on September 13, 2018, as doi:10.3324/haematol.2018.201301.

Long non-coding RNA NEAT1 shows high expression unrelated to molecular features and clinical outcome in multiple myeloma

by Elisa Taiana, Domenica Ronchetti, Vanessa Favasuli, Katia Todoerti, Martina Manzoni, Nicola Amodio, Pierfrancesco Tassone, Luca Agnelli, and Antonino Neri

Haematologica 2018 [Epub ahead of print]

Citation: Elisa Taiana, Domenica Ronchetti, Vanessa Favasuli, Katia Todoerti, Martina Manzoni, Nicola Amodio, Pierfrancesco Tassone, Luca Agnelli and Antonino Neri. Long non-coding RNA NEAT1 shows high expression unrelated to molecular features and clinical outcome in multiple myeloma.
Haematologica. 2018; 103:xxx
doi:10.3324/haematol.2018.201301

Long non-coding RNA NEAT1 shows high expression unrelated to molecular features and clinical outcome in multiple myeloma

Elisa Taiana,[1,2*] Domenica Ronchetti,[1,2*] Vanessa Favasuli,[1,2] Katia Todoerti,[1,2] Martina Manzoni,[1,2] Nicola Amodio,[3] Pierfrancesco Tassone,[3,4] Luca Agnelli, [1,2] Antonino Neri[1,2]

[1]Department of Oncology and Hemato-oncology, University of Milan, Italy
[2]Hematology, Fondazione Cà Granda IRCCS Policlinico, Milan, Italy
[3]Department of Experimental and Clinical Medicine, Magna Graecia University of Catanzaro, Catanzaro, Italy
[4]Sbarro Institute for Cancer Research and Molecular Medicine, Center for Biotechnology, College of Science and Technology, Temple University, Philadelphia, PA, US

*These authors equally contributed to the work

Corresponding author:

Antonino Neri, MD, PhD

Dept. of Oncology and Hemato-oncology

Università degli Studi di Milano

Via Santa Sofia 9, 20122 Milano, Italy

Phone: +39 02-50320420

Fax: +39 02-50320403

e-mail: antonino.neri@unimi.it

Running title: NEAT1 in multiple myeloma

Key words: NEAT1, multiple myeloma, lncRNA

Dear Editor

The knowledge of lncRNAs in multiple myeloma (MM) is continuously increasing.[1, 2] We and others have recently provided evidence by microarray[3] or RNA sequencing (RNA-seq) analyses[2, 4] that distinct lncRNA transcriptional signatures distinguished myeloma cells from normal counterpart, were specifically associated with molecular subgroups or progressive disease phases, and could be independently related to MM clinical outcome.[4] Among the most expressed lncRNAs, we identified the nuclear paraspeckle assembly transcript 1 (NEAT1),[2] already reported to be overexpressed in many types of solid tumors, raising the hypothesis that it may play a critical oncogenic role and facilitate tumorigenesis.[5] Herein, we demonstrated that MM cells significantly overexpress NEAT1 and its deregulation is unrelated to the patients' prognosis. However, the putative NEAT1 involvement in cellular stress response makes it an attractive candidate for targeted therapy in the disease.

The expression profile of NEAT1 has been primarily investigated by GeneChip® Human Gene 2.0 ST array in a cohort of 50 MMs representative of the major molecular characteristics of the disease (Supplementary Table S1), in 9 primary plasma cell leukemia (pPCL) and 6 secondary PCL (sPCL), and in 4 purified bone marrow PCs from healthy controls (N). Almost 19000 coding genes and 10138 lncRNAs have been annotated based on the GENCODE encyclopedia as previously described.[3] NEAT1 belonged to a short list of 17 lncRNAs markedly expressed in MM patients (Supplementary Table S2). NEAT1 presents two isoforms: a canonically polyadenylated short transcript of 3.7 kb (NEAT1_1) and a longer non-polyadenylated transcript (NEAT1_2) of about 23 kb. The analysis indicated that NEAT1 showed significant overexpression in pathological MM and both pPCL and sPCL samples as compared with healthy donors (Figure 1A). Notably, MM patients overexpressed NEAT1 irrespectively of their molecular characteristic, i.e. the presence of chromosomal translocations, hyperdiploidy, 13q and 17p13 deletion, gain of 1q arm, mutations of

the MAPK-pathway (*BRAF*, *NRAS*, or *KRAS*), or *FAM46C* and *DIS3* genes (Figure 1B and Supplementary Figure S1).

Subsequently, we evaluated the expression of NEAT1 in 30 of the 50 MM patients for whom RNA-seq data were available[2] (Figure 1C). RNA-seq allowed to estimate NEAT1_1 and NEAT1_2 isoforms abundance based on the presence of unambiguously mapped reads. Importantly, we found that NEAT1_1 isoform was much more abundant than the longer NEAT1_2 isoform, being approximately 90% of total NEAT1 abundance (Figure 1D). The results on these 30 patients, representative of the major genetic/prognostic lesions, confirmed that NEAT1 is not differentially expressed in the diverse MM molecular subtypes.[2]

NEAT1 expression levels were therefore validated by quantitative real-time PCR (qRT-PCR, Supplementary Table S3) in 60 (46 MM and 14 PCL) of the pathological samples examined by arrays and in 46 additional patients including 36 MM, 5 smoldering MM, 5 PCL. NEAT1 global expression levels were first obtained by targeting the 5'-region, to amplify both transcripts. The expression pattern observed was consistent with the array results (Supplementary Figure S2). Furthermore, we used a second primers configuration that targeted the 3'-region, to amplify exclusively the NEAT1_2 isoform. As such, we confirmed the estimated proportion of NEAT1_2 in the overall NEAT1 expression as shown by RNA-seq and proved that the long isoform NEAT1_2 was positively correlated with total NEAT1 (Figure 1E). No differential expression was found in the small subset of smoldering MM (Supplementary Figure S3), in line with previous observations that indicated lack of significant differences in pathological specimens. Next, we validated these findings in two publicly available array-based datasets from the University of Arkansas for Medical Science (UAMS), including 22 healthy donors, 12 monoclonal gammopathy of undetermined significance (MGUS), 44 smoldering MM (#GSE5900 series on NCBI GEO repository) and the large array-profiled UAMS TT2/TT3 trials cohort encompassing more than 550 patients (#GSE2658 and #GSE24080). Underexpression of NEAT1 was confirmed in healthy donors; NEAT1 levels were also significantly reduced in MGUS patients compared to MM (Supplementary

Figure S4). However, for the sake of clarity, it is worth specifying that these datasets, given the related array configuration, investigated preferentially the short polyadenylated NEAT1_1 isoform.

To gain insights into the possible role of deregulated NEAT1 in MM, we investigated the protein-coding genes concurrently detected by Gene 2.0 ST array. NEAT1 is an indispensable structural component of paraspeckles (PSs), peculiar lncRNA-directed nuclear bodies potentially involved in stress response. Although their exact function has to be fully elucidated, PSs may affect gene expression by regulating the transcription and pre-mRNA splicing events and holding nuclear mRNA for editing. NEAT1 could control these events by modulating the functions of PSs upon exposure to specific stress events.[6-8] Notably, in our cohort of sample NEAT1 expression is significantly correlated with that of *NONO* and *SFPQ* (Pearson correlation $R>0.3$, $p<0.01$, Supplementary Figure S5), both encoding for proteins essential to the formation of minimal ribonucleoprotein particles.[9] These data suggest that NEAT1 overexpression in MM may be associated with increased PSs formation.

With NEAT1 being expressed at high level in all tumor samples but presenting low variance across the whole dataset, we focused on those patients at the extremes of the expression distribution to unravel putative biological effects associated with its modulation. Namely, we compared the transcriptional profiles of patients showing the highest and the lowest quartile of NEAT1 expression levels, obtaining 138 differentially expressed genes (Supplementary Table S4). Functional annotation analysis of this signature, aimed at identifying highly significant represented categories, interestingly revealed enrichment in the unfolded protein response (UPR) category, which is the cellular response to the endoplasmic reticulum stress due to the accumulation of unfolded or misfolded proteins (Supplementary Table S5). Specifically, among the 7 genes included in this gene set (*BAG3*, *EXOSC2*, *TUBB2A*, *DDX10*, *PREB*, *NFYA*, *GEMIN4*), MM with the highest NEAT1 transcript levels underexpressed all of them but *BAG3*. Since persistent activation of UPR in MM leads to apoptosis,[10] the down-modulation of UPR pathway genes might suggest a survival attempt for myeloma cells. Furthermore, the functional enrichment analysis indicated that higher NEAT1

expression was associated with lower expression of *DYNLL1*, essential for p53 nuclear trafficking, with consequent transcriptional activation of genes involved in growth arrest and apoptosis in response to DNA damage.[11] Consistently with reduced amount of p53 dynein-dependent nuclear translocation, enrichment analysis using GSEA tool evidenced that higher NEAT1 expression was correlated with weakened DNA repair-associated pathways. GSEA identified also enrichment in pathways associated with DNA synthesis and repair in MM with lower NEAT1 levels, and PI3K/AKT activation pathway in patients with high NEAT1 expression (Figure 2), in agreement with recent data describing NEAT1 as crucial player in suppressing transformation in response to oncogenic signals.[12] For completeness, GSEA analysis was run in the #GSE2658 series, which confirmed significance in PI3KT/AKT activation pathway (Supplementary Table S6).

Subsequently, we found that high NEAT1 expression was associated with 27 overexpressed and 2 underexpressed lncRNA transcripts (Figure 3 and Supplementary Table S7). Although most of these are virtually uncharacterized, three overexpressed ncRNAs, namely the two miRNA precursors MIR22HG and MIR29A, and C3orf35 (Figure 3), have been already reported in the context of MM. In particular, MIR22HG located at 17p13 was underexpressed in different solid tumors[13] and in MM.[4] It produces the mature miR-22, positively associated with progression free survival (PFS) in pPCL.[14] In our cohort of patients, no differences in MIR22HG expression were appreciable among healthy donors, MM and PCL samples. MIR29A, mapped at 7q32, was overexpressed in MM showing the highest NEAT1 level. From MIR29A originate 2 miRNAs, miR-29a and miR-29b-1, whose tumor suppressor activities have been well documented in MM.[15] With regard to the expression levels of lncRNA, no significant differences were evidenced between MIR29A expression in healthy and pathological samples, the latter showing very heterogeneous expression pattern. Finally, C3orf35, mapped at 3p22, was recently described as overexpressed in MM versus normal control,[4] although this data was not confirmed in our microarray dataset.

To evaluate the potential prognostic value of NEAT1 in MM, we analyzed a retrospectively collected proprietary dataset including 55 MM at diagnosis for whom clinical data were available,

over a median follow-up of 54 months. In particular, we assessed the expression of both global NEAT1 gene and the longer NEAT1_2 transcript separately by qRT-PCR, both of them correlated with neither overall survival nor the time to next treatment (Supplementary Table S8). Furthermore, we extended the qRT-PCR analysis to 12 additional MM patients (seven of them included in the 55-sample dataset) for whom we had serial samples at the onset and relapse, but even in this case no significant variation in NEAT1 expression was observed (Supplementary Figure S6). Finally, we evaluated the NEAT1 prognostic significance in the TT2/TT3 trials cohort, showing no significant correlation between NEAT1_1 isoform expression and OS (Supplementary Figure S7).

In conclusion, MM significantly overexpresses NEAT1, although, based on the available data, its deregulation appears do not directly affect the patient's prognosis. However, the putative NEAT1 involvement in different mechanisms of cellular stress response, such as the UPR and p53 pathways, makes it a confident candidate for further studies in a perspective of targeted therapy in the disease.

Acknowledgements

This work was financially supported by grants from Associazione Italiana Ricerca sul Cancro (AIRC) to Antonino Neri (IG16722, IG10136, and the "Special Program Molecular Clinical Oncology-5 per mille" #9980, 2010/15); Elisa Taiana was supported by a fellowship (#19370) from Fondazione Italiana Ricerca sul cancro (FIRC); Katia Todoerti was supported by a fellowship from Fondazione Umberto Veronesi.

Conflict of interest

The authors declare no conflict of interest.

References

1. Nobili L, Ronchetti D, Agnelli L, Taiana E, Vinci C, Neri A. Long Non-Coding RNAs in Multiple Myeloma. Genes (Basel). 2018;9(2).
2. Ronchetti D, Agnelli L, Pietrelli A, et al. A compendium of long non-coding RNAs transcriptional fingerprint in multiple myeloma. Sci Rep. 2018;8(1):6557.
3. Ronchetti D, Agnelli L, Taiana E, et al. Distinct lncRNA transcriptional fingerprints characterize progressive stages of multiple myeloma. Oncotarget. 2016;7(12):14814-14830.
4. Samur MK, Minvielle S, Gulla A, et al. Long intergenic non-coding RNAs have an independent impact on survival in multiple myeloma. Leukemia. 2018 Mar 29. [Epub ahead of print]
5. Yu X, Li Z, Zheng H, Chan MT, Wu WK. NEAT1: A novel cancer-related long non-coding RNA. Cell Prolif. 2017;50(2).
6. Adriaens C, Standaert L, Barra J, et al. p53 induces formation of NEAT1 lncRNA-containing paraspeckles that modulate replication stress response and chemosensitivity. Nat Med. 2016;22(8):861-868.
7. Naganuma T, Hirose T. Paraspeckle formation during the biogenesis of long non-coding RNAs. RNA Biol. 2013;10(3):456-461.
8. Naganuma T, Nakagawa S, Tanigawa A, Sasaki YF, Goshima N, Hirose T. Alternative 3'-end processing of long noncoding RNA initiates construction of nuclear paraspeckles. EMBO J. 2012;31(20):4020-4034.
9. Fox AH, Nakagawa S, Hirose T, Bond CS. Paraspeckles: Where Long Noncoding RNA Meets Phase Separation. Trends Biochem Sci. 2018;43(2):124-135.
10. Woo CW, Cui D, Arellano J, et al. Adaptive suppression of the ATF4-CHOP branch of the unfolded protein response by toll-like receptor signalling. Nat Cell Biol. 2009;11(12):1473-1480.
11. Lo KW, Kan HM, Chan LN, et al. The 8-kDa dynein light chain binds to p53-binding protein 1 and mediates DNA damage-induced p53 nuclear accumulation. J Biol Chem. 2005;280(9):8172-8179.
12. Mello SS, Sinow C, Raj N, et al. Neat1 is a p53-inducible lincRNA essential for transformation suppression. Genes Dev. 2017;31(11):1095-1108.
13. Cui Z, An X, Li J, Liu Q, Liu W. LncRNA MIR22HG negatively regulates miR-141-3p to enhance DAPK1 expression and inhibits endometrial carcinoma cells proliferation. Biomed Pharmacother. 2018;104:223-228.
14. Lionetti M, Musto P, Di Martino MT, et al. Biological and clinical relevance of miRNA expression signatures in primary plasma cell leukemia. Clin Cancer Res. 2013;19(12):3130-3142.
15. Stamato MA, Juli G, Romeo E, et al. Inhibition of EZH2 triggers the tumor suppressive miR-29b network in multiple myeloma. Oncotarget. 2017;8(63):106527-106537.

Figure Legends

Figure 1: NEAT1 expression by GeneChip® Human Gene 2.0 ST arrays. A. Boxplot of NEAT1 expression shows a significant upregulation in pathological MM, pPCL and sPCL samples as compared with healthy control based on Dunn test (* means *p*-values <0.01). **B.** Boxplot of NEAT1 expression doesn't show any significant correlation with group membership defined by t(11;14), t(4;14), MAF translocation, and hyperdiploid status. **C.** NEAT1 expression by RNA sequencing. Visualization of RNA-seq data: zoomed view of the NEAT1 lncRNA region; the coverage bigWig files generated using bamCoverage function in deeptools (http://deeptools.readthedocs.io/en/latest/content/tools/bamCoverage.html) and the human genome annotation file (GENCODE v.25) were loaded into the Integrated Genome Viewer (IGV [http://www.broadinstitute.org/igv/]. The y axis shows the scaled number of reads mapping to each location of the genome in the NEAT1 region (x axis) schematically reported below together with qRT-PCR primers. Each lane represents a MM patient: different colors refer to the sample molecular characteristic indicated at the left. In order to compare samples, coverage values from all patients were group-scaled. **D.** Boxplot of NEAT1_1 and NEAT1_2 expression by RNA-seq showing that the shorter transcript is expressed approximately 10-fold higher than the longer isoform. Transcript abundance was estimated as Fragments Per Kilobase per Million mapped reads (FPKM). **E.** Pearson analysis correlating NEAT1 total expression (x-axis) with the long transcript expression (y-axis). Correlation coefficient R and significant *p*-value are reported.

Figure 2: Functional annotation of NEAT1 signature in MM. A. Enrichment plots of four selected gene sets detected by GSEA. The green curves show the enrichment score and reflect the degree to which each gene (black vertical lines) is represented at the bottom of the ranked gene list. Genes contributing to the core enrichment (C.E.) in the gene set are indicated in bold with Y. **B.** Heatmap of the 138 differentially expressed genes identified by comparing the first vs fourth quartile of 50 MM patients stratified into four groups based on NEAT1 expression level.

Figure 3: lncRNAs differentially expressed based on NEAT1 expression. A. Heatmap of the 30 differentially expressed lncRNAs identified by comparing the first vs fourth quartile of 50 MM patients stratified into four groups based on NEAT1 expression level. **B.** Boxplot of MIR22HG, MIR29A, and C3orf35 expression levels in 4N, 50MM and 15 PCL samples profiled on GeneChip® Human Gene 2.0 ST arrays.

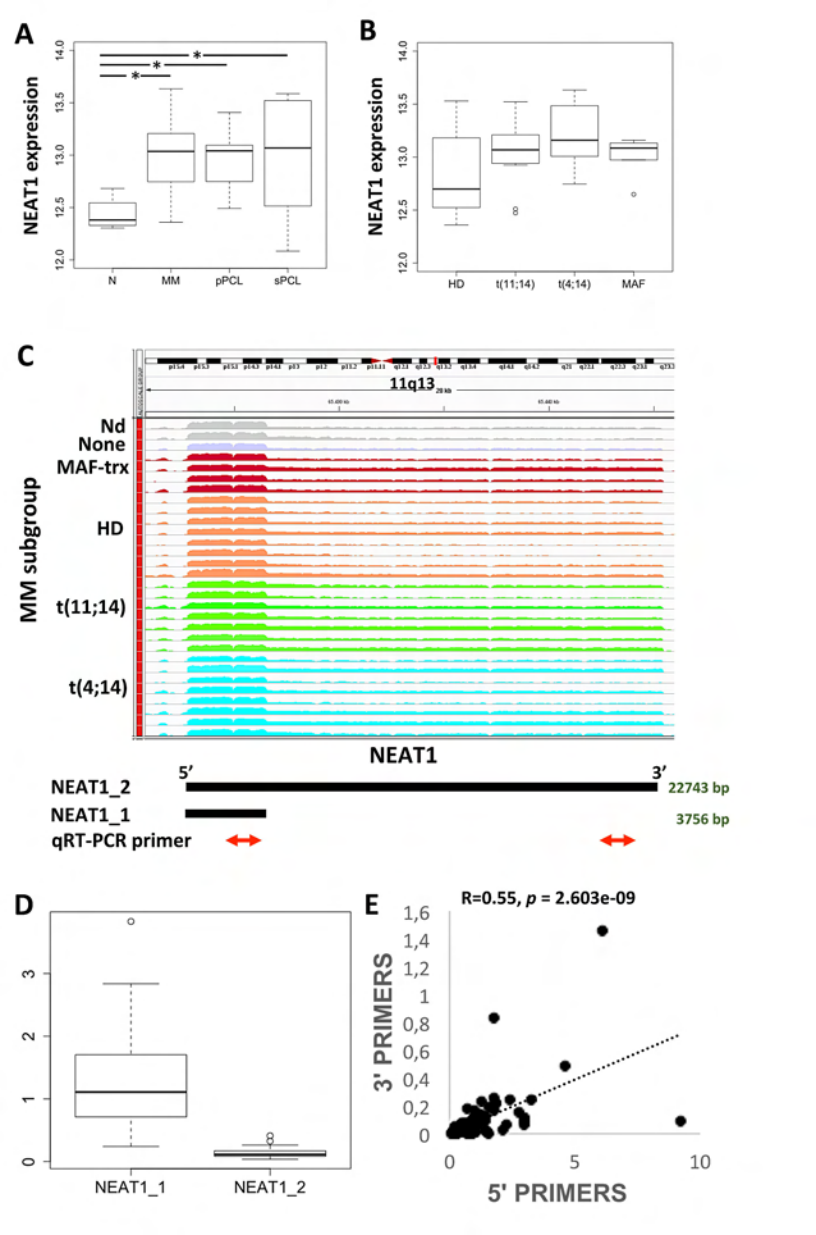
A
NEAT1 expression
14.0
13.5
13.0
12.5
12.0
*
*
*
N
MM
pPCL
sPCL
B
NEAT1 expression
14.0
13.5
13.0
12.5
12.0
HD
t(11;14)
t(4;14)
MAF
C
11q13
MM subgroup
Nd
None
MAF-trx
HD
t(11;14)
t(4;14)
NEAT1
5'
3'
NEAT1_2
22743 bp
NEAT1_1
3756 bp
qRT-PCR primer
D
3
2
1
0
NEAT1_1
NEAT1_2
E
R=0.55, p = 2.603e-09
3' PRIMERS
1,6
1,4
1,2
1
0,8
0,6
0,4
0,2
0
0
5
10
5' PRIMERS

A

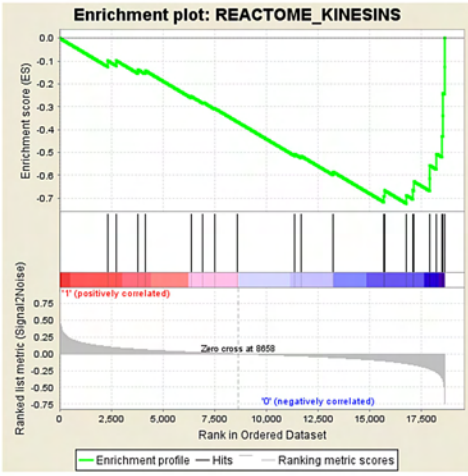

GENE	C.E.
KIF3B	N
KLC1	N
KIF5B	N
KIFAP3	N
KIF26A	N
KIF2B	N
KIF9	N
KIF2A	N
KIF4B	N
KLC3	N
KLC2	N
KIF4A	**Y**
KLC4	**Y**
KIF22	**Y**
KIF3C	**Y**
KIF5A	**Y**
KIFC1	**Y**
KIF2C	**Y**
KIF18A	**Y**
KIF11	**Y**
KIF20A	**Y**
KIF23	**Y**
RACGA	**Y**
KIF15	**Y**

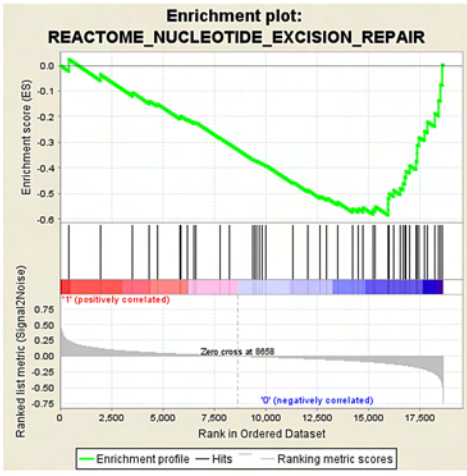

GENE	C.E.	GENE	C.E.
GTF2H4	N	POLR2K	N
TCEA1	N	RFC3	N
RFC5	N	**RFC2**	**Y**
RAD23B	N	**ERCC6**	**Y**
POLR2A	N	**ERCC1**	**Y**
CDK7	N	**LIG1**	**Y**
ERCC5	N	**RPA2**	**Y**
XPA	N	**ERCC2**	**Y**
POLR2B	N	**POLD1**	**Y**
POLR2D	N	**POLD2**	**Y**
ERCC4	N	**POLE**	**Y**
XAB2	N	**POLD4**	**Y**
XPC	N	**POLD3**	**Y**
DDB1	N	**POLR2H**	**Y**
CCNH	N	**POLR2E**	**Y**
POLR2J	N	**RPA3**	**Y**
POLR2F	N	**GTF2H1**	**Y**
ERCC3	N	**MNAT1**	**Y**
POLR2L	N	**RFC4**	**Y**
POLR2C	N	**DDB2**	**Y**
POLR2G	N	**POLE2**	**Y**
GTF2H3	N	**RPA1**	**Y**
ERCC8	N	**PCNA**	**Y**
POLR2I	N	**GTF2H2**	**Y**

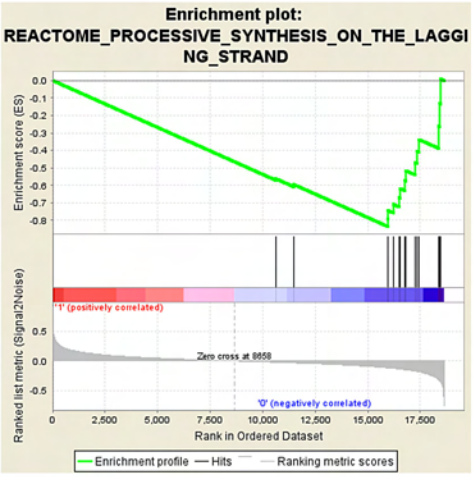

GENE	C.E.
FEN1	**N**
DNA2	**N**
LIG1	**Y**
RPA2	**Y**
POLD1	**Y**
POLA1	**Y**
POLD2	**Y**
POLD4	**Y**
POLD3	**Y**
PRIM2	**Y**
RPA3	**Y**
POLA2	**Y**
RPA1	**Y**
PRIM1	**Y**
PCNA	**Y**

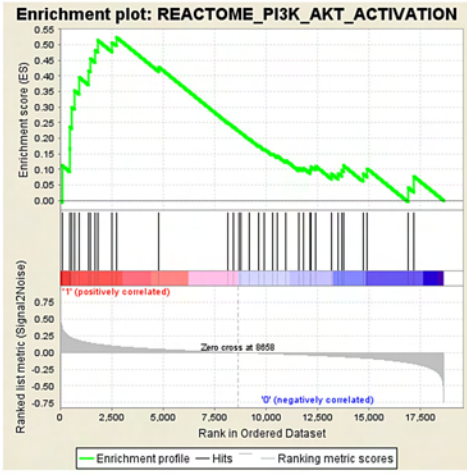

GENE	C.E.	GENE	C.E.
AKT3	**Y**	FOXO4	N
PIK3CA	**Y**	NGF	N
PHLPP1	**Y**	MLST8	N
IRS1	**Y**	CREB1	N
IRS2	**Y**	BAD	N
CDKN1A	**Y**	PDPK1	N
CHUK	**Y**	MTOR	N
NR4A1	**Y**	FOXO3	N
CDKN1B	**Y**	RPS6KB2	N
RICTOR	**Y**	AKT2	N
FOXO1	**Y**	PIK3CB	N
TRIB3	**Y**	GSK3A	N
NTRK1	N	TSC2	N
MDM2	N	MAPKAP	N
AKT1	N	AKT1S1	N
RHOA	N	THEM4	N
CASP9	N	PIK3R2	N
PIK3R1	N	PTEN	N

B

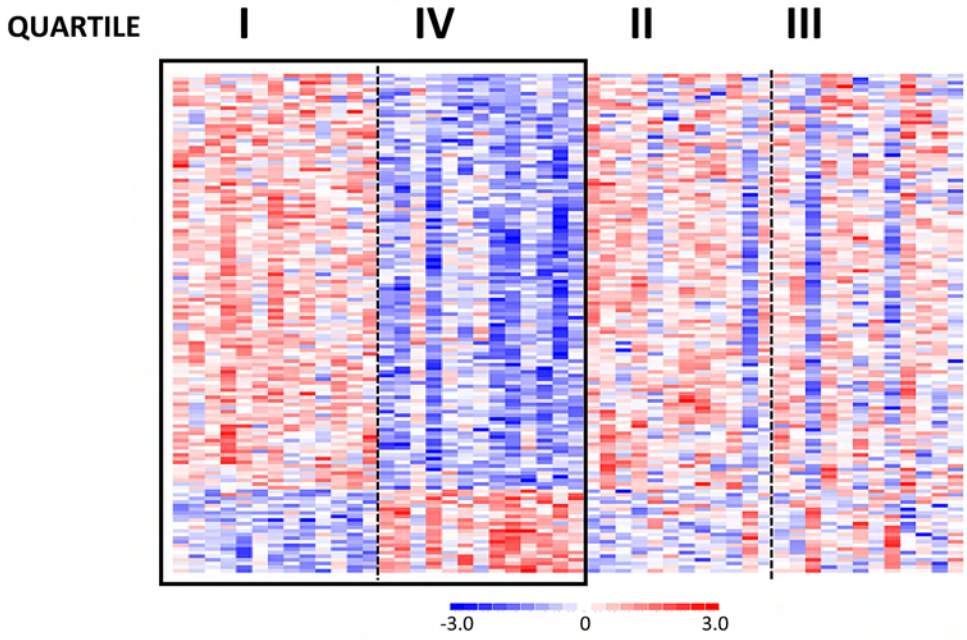

A

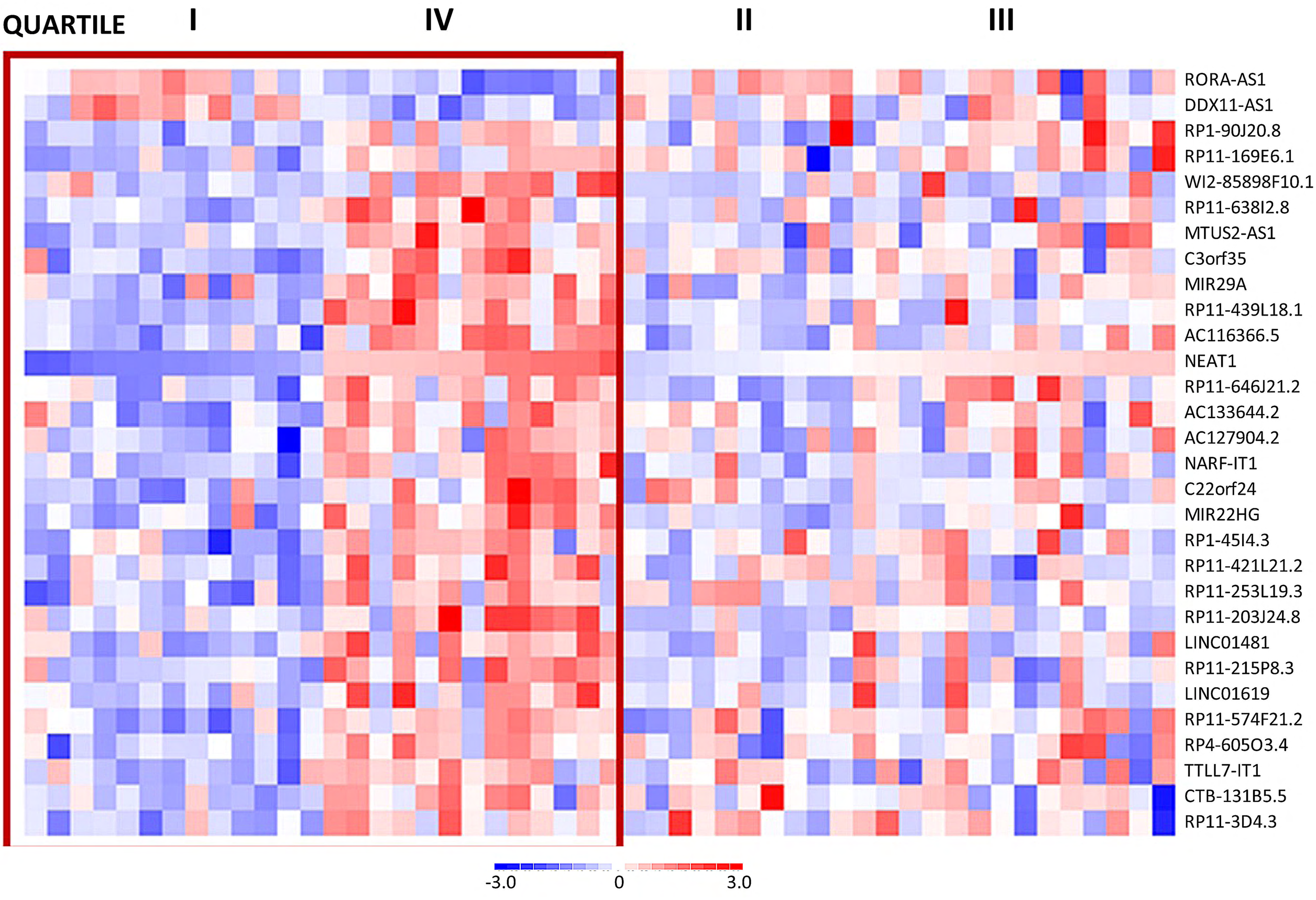
QUARTILE
I
IV
II
III
RORA-AS1
DDX11-AS1
RP1-90J20.8
RP11-169E6.1
WI2-85898F10.1
RP11-638I2.8
MTUS2-AS1
C3orf35
MIR29A
RP11-439L18.1
AC116366.5
NEAT1
RP11-646J21.2
AC133644.2
AC127904.2
NARF-IT1
C22orf24
MIR22HG
RP1-45I4.3
RP11-421L21.2
RP11-253L19.3
RP11-203J24.8
LINC01481
RP11-215P8.3
LINC01619
RP11-574F21.2
RP4-605O3.4
TTLL7-IT1
CTB-131B5.5
RP11-3D4.3
-3.0
0
3.0

B

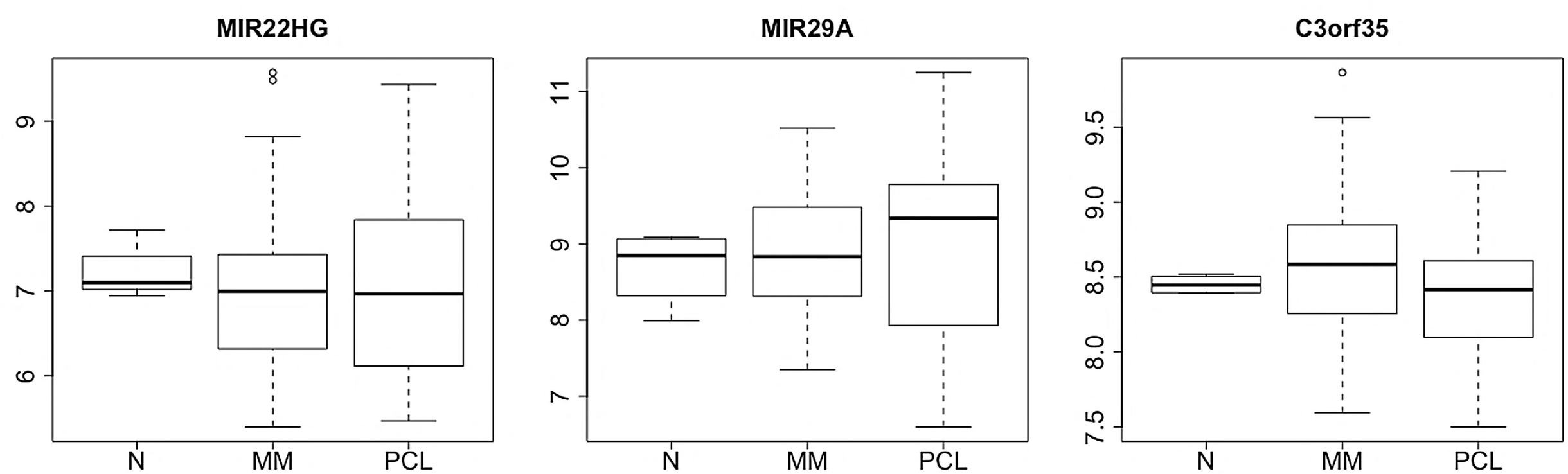
MIR22HG
MIR29A
C3orf35
N
MM
PCL
N
MM
PCL
N
MM
PCL

Supplementary Materials

Long non-coding RNA NEAT1 shows high expression unrelated to molecular features and clinical outcome in multiple myeloma

Elisa Taiana,[1,2*] Domenica Ronchetti,[1,2*] Vanessa Favasuli,[1,2] Katia Todoerti, [1,2] Martina Manzoni,[1,2] Nicola Amodio,[3] Pierfrancesco Tassone,[3,4] Luca Agnelli, [1,2] Antonino Neri[1,2]

[1]Department of Oncology and Hemato-oncology, University of Milan, Italy
[2]Hematology, Fondazione Cà Granda IRCCS Policlinico, Milan, Italy
[3]Department of Experimental and Clinical Medicine, Magna Graecia University of Catanzaro, Catanzaro, Italy
[4]Sbarro Institute for Cancer Research and Molecular Medicine, Center for Biotechnology, College of Science and Technology, Temple University, Philadelphia, PA, US

Corresponding author:

Antonino Neri, MD, PhD

Fax: +39 02-50320403

e-mail: antonino.neri@unimi.it

Supplementary Materials and Methods

Samples

We investigated a cohort of 50 MM patients representative of the major molecular characteristics of the disease, 9 primary PCLs (pPCL) and 6 secondary PCLs (sPCL) and four normal controls (purchased from Voden, Medical Instruments IT) (Table 1). PCs (>90%) were purified from bone marrow aspirates using CD138 immunomagnetic microbeads (MidiMACS system, Miltenyi Biotec, Auburn, CA). All the samples were characterized by fluorescence in situ hybridization (FISH) for the ploidy status and the presence of 17p13 or 13q14 deletions, 1q gain and the most frequent IGH chromosomal translocations t(11;14), t(4;14), t(14;16) and t(14;20), as previously described.[1] The mutations pattern of *BRAF*, *NRAS*, *KRAS*, *P53*, *FAM46C* and *DIS3* genes have been previously investigated by next-generation sequencing.[2-4] Written informed consent was obtained from all patients in accordance with the declaration of Helsinki. The study was approved by the Ethical Committee of the University of Milan (N° 24/15, May 06 2015).

Gene Expression Profiling

All MM and PCL patients along with the 4 BM PC normal controls were profiled on GeneChip® Human Gene 2.0 ST arrays (Affymetrix Inc., Santa Clara, CA). Total RNA samples were processed according to manufacturer's procedure. Normalized expression values were obtained using Robust Multi Array Average (RMA) procedure and annotations based on GENCODE v25, Ensembl v87 (Chip Definition File available at http://brainarray.mbni.med.umich.edu/Brainarray/Database/CustomCDF/21.0.0/genecodet.asp). CDF file was customized in order to withdraw probes that map to regions where ambiguous detection due to transcript overlap might occur. In this way, the expression levels of 10138 unique lncRNAs were obtained. The list of differentially expressed genes or lncRNAs between high and low *NEAT1* expressing samples was gathered by Significant Analysis of Microarrays v5.00, using the tool provided for the *shiny* package in R software (https://github.com/MikeJSeo/SAM), as previously described.[5]

The list of differentially expressed genes was submitted to the ToppGene Suite portal (http://toppgene.cchmc.org) for functional enrichment analysis using the ToppFun application. Microarray data were globally analyzed by Gene Set Enrichment Analysis (GSEA, software v.2.2.1).[6] Gene sets were considered significant with nominal p-value < 0.05. All the data have been deposited in the NCBI Gene Expression Omnibus database (GEO; http//www.ncbi.nlm.nih.gov/geo) and are accessible under accession #GSE116294.

RNA sequencing (RNA-seq)

The sequencing data have been previously generated and were publicly available at GEO repository under accession #GSE109342. Transcript abundance was estimated as previously described [7] and was reported as FPKM, Fragments Per Kilobase per Million mapped reads. *Cufflinks* estimates a likelihood of relative abundances for all the possible sets of transcripts based on the identified 'incompatible' fragments that stemmed from differently spliced mRNA isoforms, producing a numerical value that best explains the observed fragments.

Quantitative real-time PCR (qRT-PCR)

For qRT-PCR, 100 ng of total RNA underwent reverse transcription using random primer mix and reagents from INVITROGEN (Life Technologies, Foster City, CA). Real-time PCR to validate NEAT1 was performed using 10 ng of total RNA and SYBR™ Green master mix with custom primers (Supplementary Table S3) as previously described. [5]

Statistical analysis

Conventional statistical tests were applied as reported in the manuscript using standard functions in base R package (Kendall Tau correlation, Pearson correlation, Dunn test, and Wilcoxon rank-sum tests).

We used the Cox proportional hazards model in the *globaltest* function of R software (with 100,000 permutation) to test the association between NEAT1 expression levels, assumed as continuous variables and overall survival (OS) or time to next treatment (TNT) as clinical outcome.

1. Agnelli L, Fabris S, Bicciato S, et al. Upregulation of translational machinery and distinct genetic subgroups characterise hyperdiploidy in multiple myeloma. *British journal of haematology.* 2007;136(4):565-573.
2. Lionetti M, Barbieri M, Manzoni M, et al. Molecular spectrum of TP53 mutations in plasma cell dyscrasias by next generation sequencing: an Italian cohort study and overview of the literature. *Oncotarget.* 2016;7(16):21353-21361.
3. Lionetti M, Barbieri M, Todoerti K, et al. A compendium of DIS3 mutations and associated transcriptional signatures in plasma cell dyscrasias. *Oncotarget.* 2015;6(28):26129-26141.
4. Lionetti M, Barbieri M, Todoerti K, et al. Molecular spectrum of BRAF, NRAS and KRAS gene mutations in plasma cell dyscrasias: implication for MEK-ERK pathway activation. *Oncotarget.* 2015;6(27):24205-24217.
5. Ronchetti D, Agnelli L, Taiana E, et al. Distinct lncRNA transcriptional fingerprints characterize progressive stages of multiple myeloma. *Oncotarget.* 2016;7(12):14814-14830.
6. Subramanian A, Tamayo P, Mootha VK, et al. Gene set enrichment analysis: a knowledge-based approach for interpreting genome-wide expression profiles. *ProcNatlAcadSciUSA.* 2005;102(43):15545-15550.
7. Ronchetti D, Agnelli L, Pietrelli A, et al. A compendium of long non-coding RNAs transcriptional fingerprint in multiple myeloma. *Scientific reports.* 2018;8(1):6557.
8. Tusher VG, Tibshirani R, Chu G. Significance analysis of microarrays applied to the ionizing radiation response. ProcNatlAcadSciUSA. 2001;98(9):5116-5121.

Supplementary Figure S1. Boxplot of NEAT1 expression does not show any significant correlation with group membership defined by deletions of chromosome 13q, 17p13, and gain of chromosome 1q, the presence of mutations of the MAPK-pathway (*BRAF*, *NRAS*, or *KRAS*), *DIS3* or *FAM46C*.

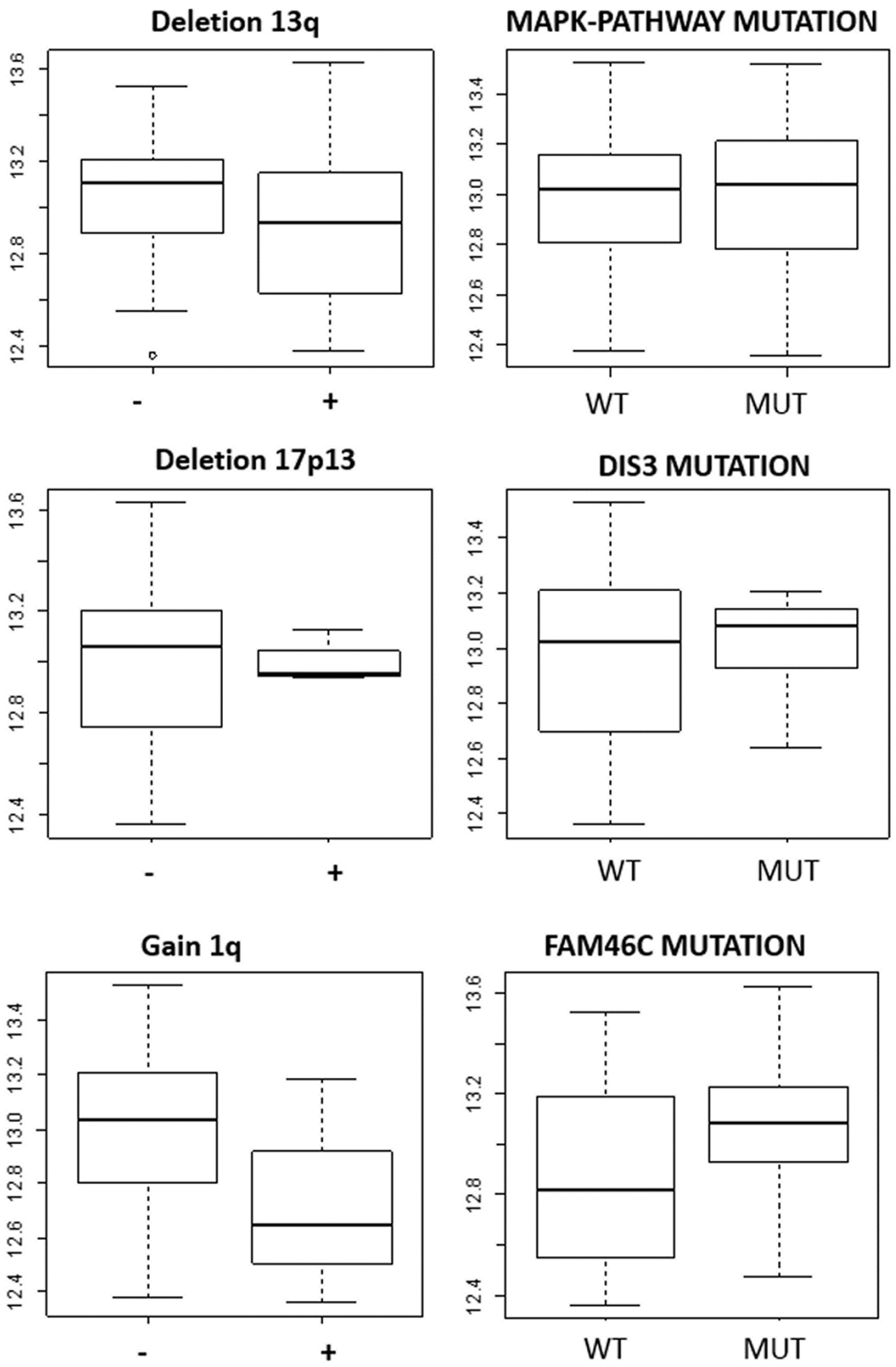

Supplementary Figure S2. A. Validation of GEP results by qRT-PCR with the 5'-primers. PCR data are represented by grouped-columns with the $2^{-\Delta Ct}$ scale on the right side; GEP data are reported as histogram with the corresponding log-scale at the left side, the dotted tendency line is also indicated. **B.** Validation of RNA-seq data by qRT-PCR with the 5'-primers. PCR data are represented by grouped-columns with the $2^{-\Delta Ct}$ scale on the right side; RNA-seq data are reported as histogram with the corresponding scale at the left side. For both graphs, Kendall coefficient and significance are reported.

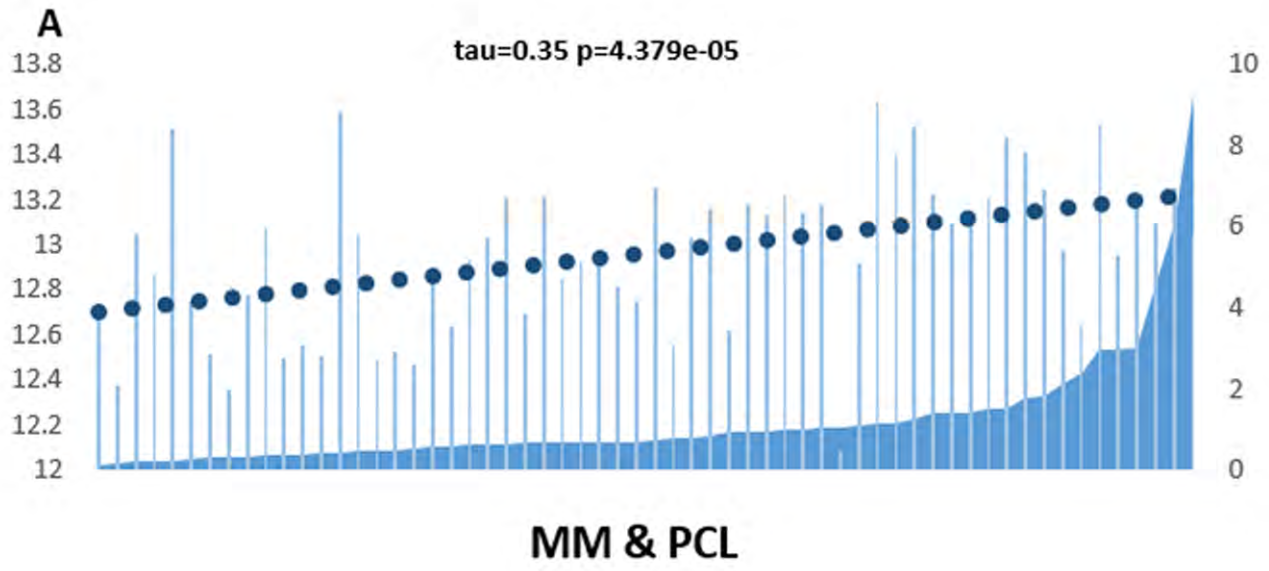

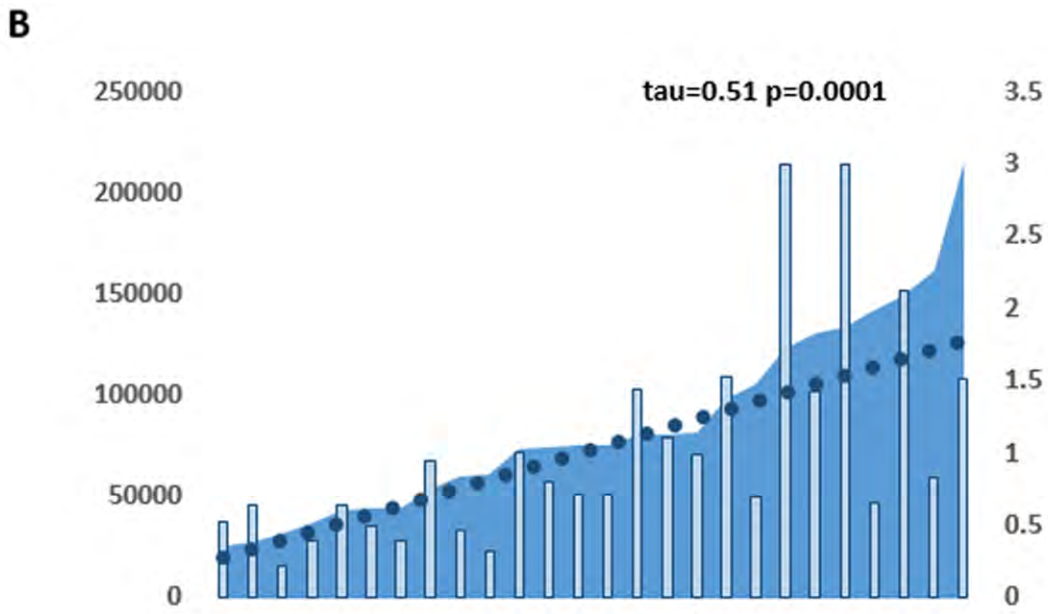

Supplementary Figure S3. Boxplot of NEAT1 qRT-PCR expression in MM/PCL versus 5 smoldering MM samples in proprietary dataset.

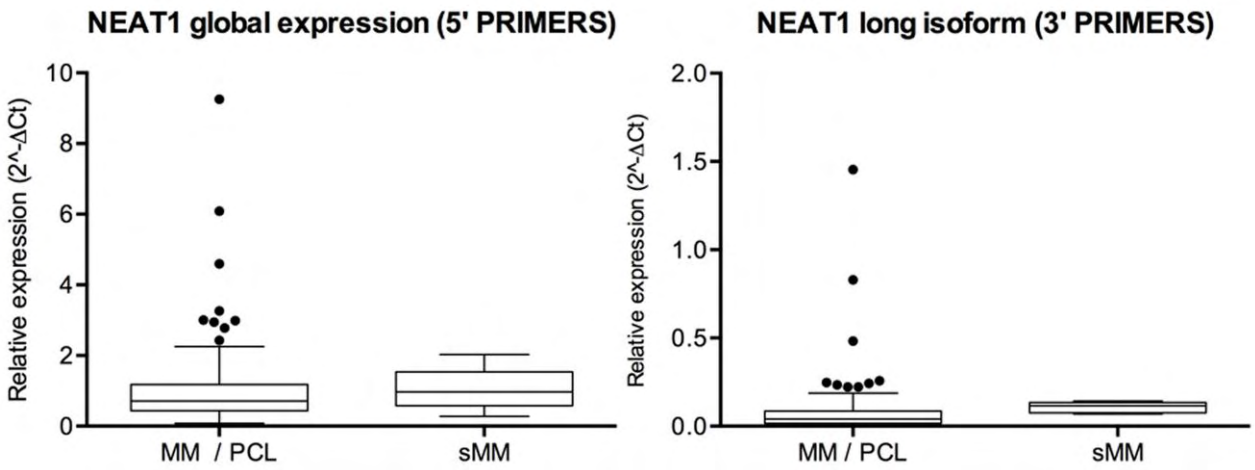

Supplementary Figure S4. Boxplot of NEAT1 isoform expression in healthy donors, MGUS, smoldering MM and MM samples from GSE5900 and GSE2658 microarray series (legend indicates Kruskal test P-value; *=Dunn's test P<0.05/2).

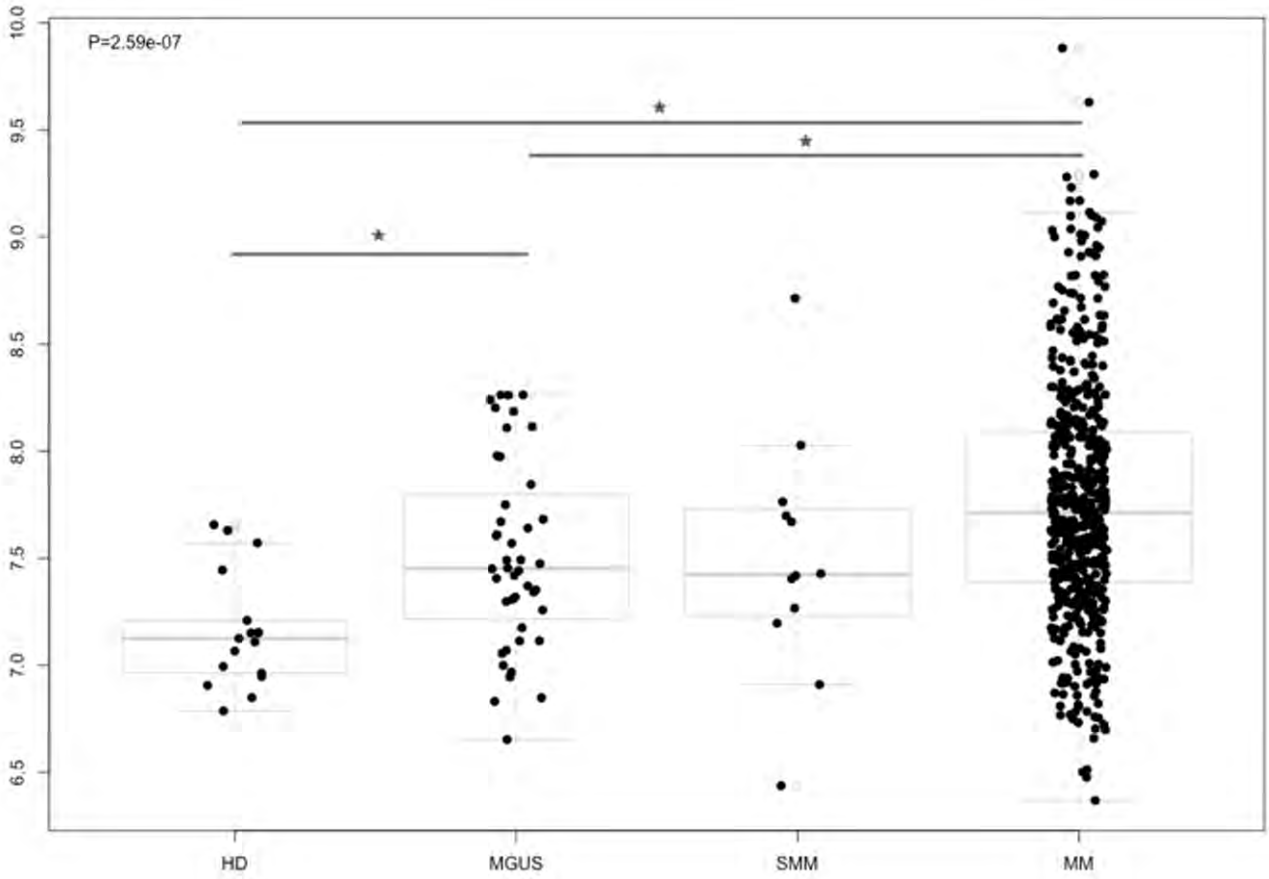

Supplementary Figure S5. Pearson analysis correlating NEAT1 total expression (x-axis) with the NONO or SFPQ (y-axis). R correlation coefficient and significance are reported.

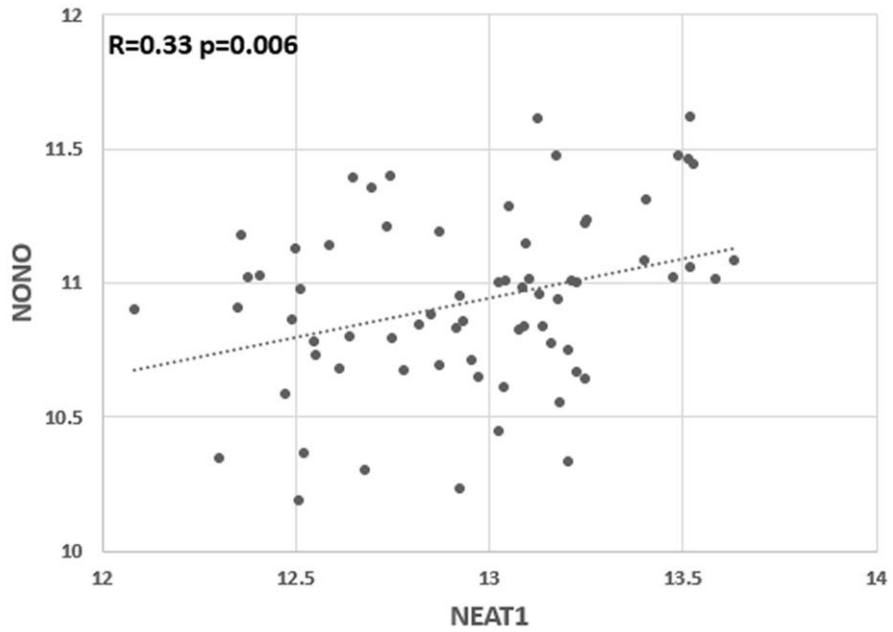

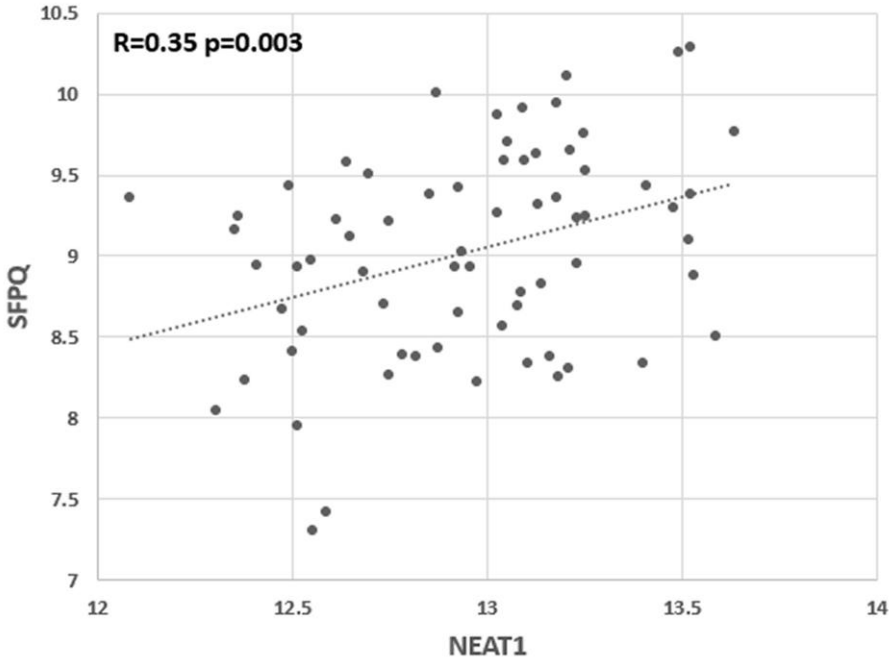

Supplementary Figure S6: Boxplot of NEAT1 qRT-PCR expression in 12 paired samples at onset and at relapse.

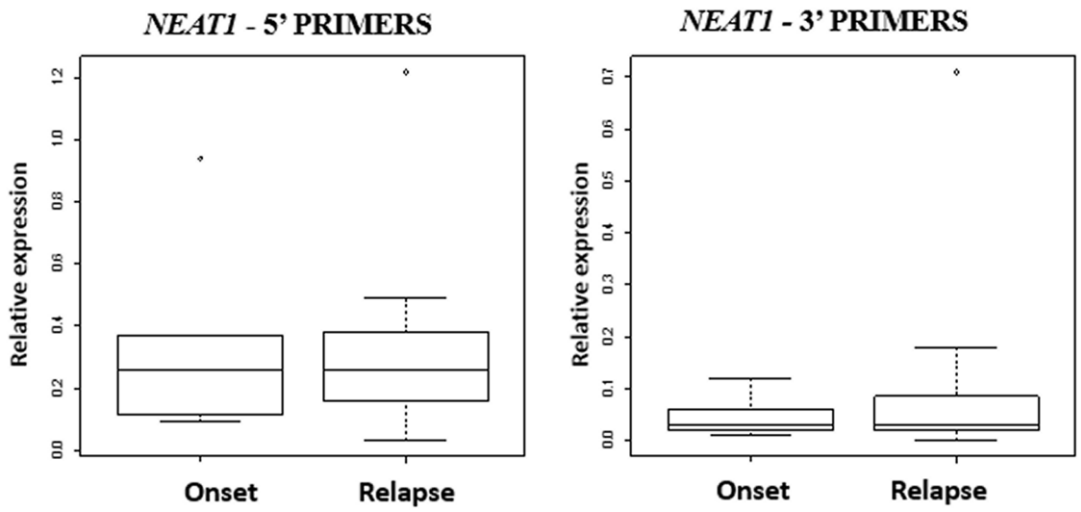

Supplementary Figure S7: Kaplan – Meier estimated curves of the two groups defined by NEAT1_1 isoform high (blue) and low (red) expression levels in GSE2658 dataset. For representation, data stratified on the median expression level are shown.

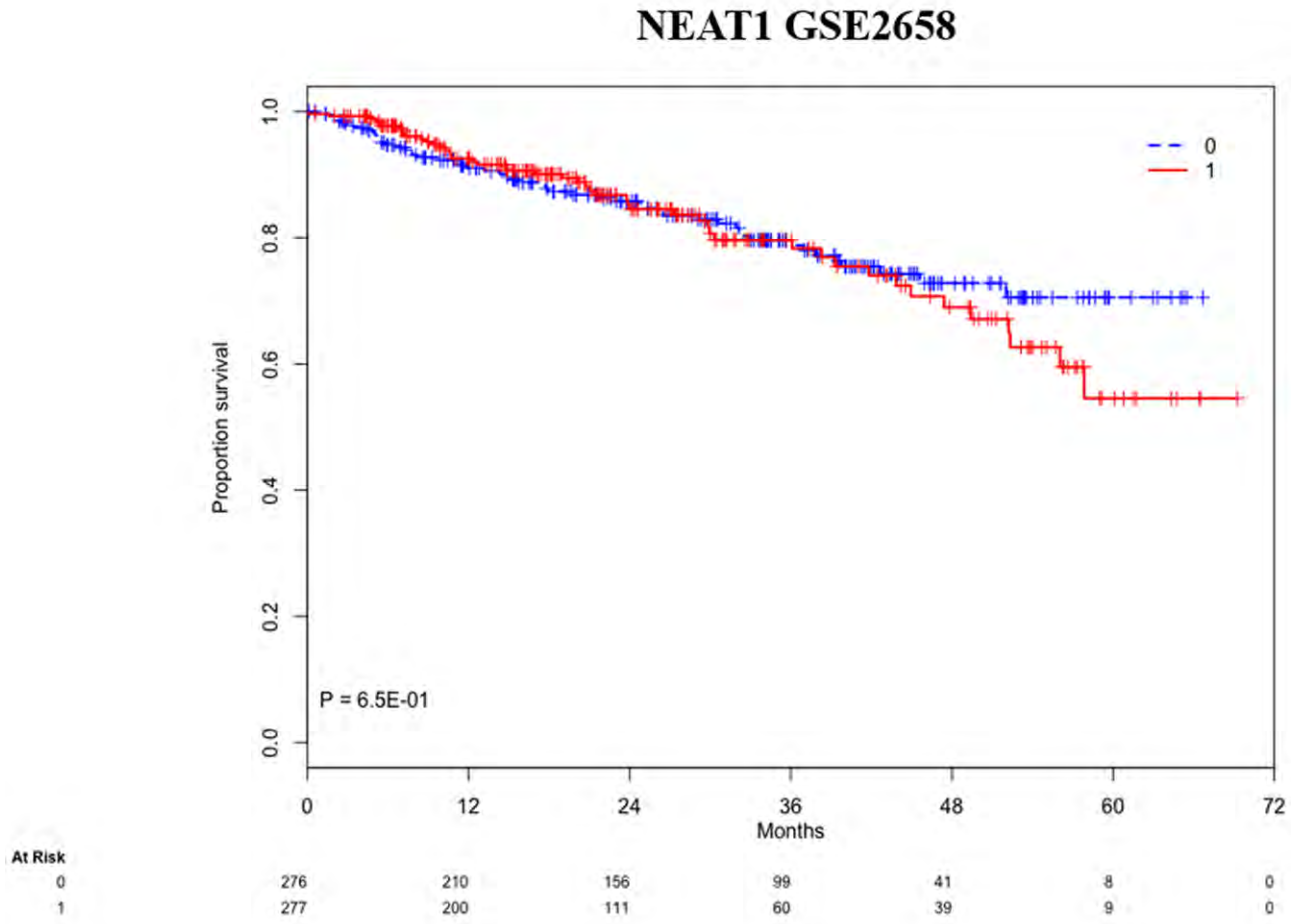

Supplementary Table S1. Molecular characteristics of 50 MM and 15 PCL patients.

	MM			PCL		
Sample Features	**Positive (%)**	**Negative (%)**	**Not available**	**Positive (%)**	**Negative (%)**	**Not available**
HD	15 (30)	32 (64)	3	0	15 (100)	0
t(11;14)	12 (24)	38 (76)	0	3(20)	12(80)	0
t(4;14)	12 (24)	38 (76)	0	3(20)	12(80)	0
MAF-trx	5 (10)	45 (90)	0	6(40)	9(60)	0
none	3 (6)	47 (94)		3(20)	12(80)	
del(17)	3 (6)	46 (92)	1	6(40)	9(60)	0
del(13)	27 (54)	23 (46)	0	9(60)	6(40)	0
1q-gain	24 (48)	20 (40)	6	7(47)	6(40)	2
N-RAS	8 (16)	33 (66)	9	1(7)	11(73)	3
K-RAS	12 (24)	29 (58)	9	1(7)	12(80)	2
BRAF	5 (10)	36 (72)	9	3(20)	10(67)	2
DIS3	9 (18)	32 (64)	9	3(20)	9(60)	3
P53	2(4)	38(76)	10	4(27)	9(60)	2
FAM46C	3(6)	36(72)	11	0	13(87)	2

Supplementary Table S2. Highly expressed lncRNAs displaying an average log2 expression >10.

Log2 expression >10	**chromosome**
LINC01001	11p15
NEAT1	11q13
MALAT1	11q13
RP11-658F2.8	11q13
RP11-736K20.5	11q14
LINC01089	12q24
LRRC75A-AS1-014	17p11
LINC01480	19q13
RP11-161I10.1	1q31
TUG1	22q12
AC074289.1	2p14
FGD5-AS1	3p25
RP11-325F22.2	7q22
LINC-PINT	7q32
EBLN3	9p13
FTX	Xq13
CDR1-AS	Xq27

Supplementary Table S3. Sequences of the primers used for qRT-PCR.

PRIMER	**Sequence 5' - 3'**
NEAT1 5’-region Forward	GCCTTGTAGATGGAGCTTGC
NEAT1 5’-region Reverse	GCACAACACAATGACACCCT
NEAT1 3’-region Forward	GGCCAGAGCTTTGTTGCTTC
NEAT1 3’-region Reverse	GGTGCGGGCACTTACTTACT

Supplementary Table S4. Modulated genes resulting from SAM (Significant Analysis of Microarray algorithm) analyses (*https://github.com/MikeJSeo/SAM*) comparing MM patients expressing high NEAT1 levels (IV quartile) and low NEAT1 levels (I quartile), ordered based on (d)-score. [8]

Gene Name	Score(d)	Fold Change
TEX14	4.84	5.64
LCA5	4.72	2.54
LRRC39	4.71	3.57
TRAF6	4.61	1.94
FAM160B1	4.58	2.26
BAG3	4.55	2.35
RIPK1	4.54	1.94
CRABP2	4.45	1.89
PIK3C2B	4.43	1.82
ARID5B	4.34	3.13
TBC1D15	4.28	2.00
FBXL3	4.19	2.17
SLC39A1	4.19	1.46
ATP13A3	4.16	1.91
UBE2B	4.14	1.84
MAD2L2	4.09	1.64
DYRK1A	4.09	2.33
GORAB	4.02	1.96
ZNF460	4.00	1.72
C16orf72	3.98	1.61
WDR26	3.97	2.30
DCAF8	3.96	1.89
CASP7	3.94	1.95
SMYD4	-5.57	0.49
WDR70	-5.04	0.58
NEMP1	-4.92	0.54
CCR2	-4.90	0.18
CCDC77	-4.90	0.53
DUSP19	-4.71	0.33
GTF2H2C	-4.66	0.55
RCCD1	-4.60	0.67
SNUPN	-4.59	0.47
CBX1	-4.56	0.48
POLH	-4.51	0.36
ALDH5A1	-4.38	0.43
SPATA5	-4.29	0.62
ELMO1	-4.28	0.58
EVI2A	-4.28	0.37
USP28	-4.27	0.46
SENP8	-4.25	0.68
CEP78	-4.24	0.54

INIP	-4.23	0.55
NAPEPLD	-4.22	0.45
POC5	-4.21	0.50
RNASEH2A	-4.18	0.55
ASXL2	-4.17	0.48
METTL7A	-4.17	0.47
NCAPD2	-4.16	0.50
ELOF1	-4.15	0.55
DAXX	-4.15	0.57
ERMP1	-4.14	0.54
DNMT1	-4.14	0.41
RASA1	-4.13	0.60
CKAP5	-4.12	0.54
CLINT1	-4.10	0.64
APEH	-4.09	0.59
BTK	-4.09	0.38
ZNF260	-4.06	0.30
HACD3	-4.05	0.47
NFYA	-4.02	0.60
GEMIN4	-4.01	0.64
ASF1B	-3.99	0.44
EHBP1	-3.98	0.50
PPP5C	-3.98	0.47
SKA2	-3.98	0.44
DROSHA	-3.97	0.61
MRPL34	-3.97	0.46
IRF2	-3.94	0.49
DFFB	-3.94	0.61
SCAI	-3.94	0.52
MUM1	-3.93	0.59
TAS2R5	-3.92	0.65
SLC38A9	-3.90	0.55
DPF2	-3.89	0.55
CCR3	-3.89	0.63
RSBN1L	-3.87	0.57
TBC1D5	-3.87	0.57
DBP	-3.85	0.56
ST3GAL5	-3.83	0.43
SLC25A40	-3.82	0.53
UCP2	-3.81	0.50
RAD51C	-3.80	0.49
THYN1	-3.79	0.51
HN1L	-3.79	0.57
BAG2	-3.79	0.51
TTLL11	-3.75	0.44
LARS	-3.75	0.48
GRHPR	-3.74	0.57

TAS2R4	-3.73	0.66
DYNLL1	-3.72	0.41
MOCS2	-3.71	0.48
TYSND1	-3.71	0.69
BCS1L	-3.70	0.48
TUBB	-3.70	0.67
ABCG2	-3.69	0.21
ZNF718	-3.69	0.57
TMEM245	-3.68	0.64
ADRB2	-3.67	0.50
SKP2	-3.67	0.46
GCDH	-3.66	0.64
GATC	-3.66	0.56
KANK1	-3.65	0.37
RHOT1	-3.65	0.53
DDX10	-3.65	0.53
RACGAP1	-3.65	0.45
FARSA	-3.64	0.55
RNF145	-3.64	0.55
OSGEPL1	-3.64	0.48
CWC27	-3.63	0.65
ARHGEF3	-3.62	0.52
ODF2	-3.59	0.63
EXOSC2	-3.58	0.54
DPY30	-3.58	0.53
C9orf114	-3.57	0.52
TLR10	-3.56	0.40
CHST12	-3.56	0.54
TBCK	-3.55	0.63
TOR1B	-3.54	0.60
TUBGCP4	-3.53	0.52
RBM4B	-3.52	0.63
POLR3K	-3.52	0.46
KYAT1	-3.52	0.72
NEURL4	-3.52	0.55
PCDHGB6	-3.52	0.45
DOCK8	-3.52	0.58
HMMR	-3.50	0.48
DCAF7	-3.48	0.62
CNNM2	-3.47	0.60
MRM2	-3.47	0.71
DNAJA3	-3.46	0.54
PREB	-3.46	0.46
TMEM138	-3.45	0.56
ATP6V0E1	-3.45	0.65
C1orf186	-3.44	0.19
HIKESHI	-3.43	0.57

MRPL17	-3.43	0.58
HSH2D	-3.43	0.49
ADAM22	-3.43	0.37

Supplementary Table S5. List of the significantly enriched Gene sets for the 138 differentially expressed genes, by ToppGene suite analysis. Q-value calculated according to Benjamini&Hochberg correction.

Category	Source	ID	Name	*q*-value	Hit Count in Query List	Hit Count in Genome	Hit in Query List
Drug	CTD	ctd:D003375	Coumestrol	3.26E-04	32	1796	RAD51C,MRM2,NEMP1,ATP6V0E1,RASA1,RNASEH2A,RCCD1,DOCK8,BAG3,BAG2,CKAP5,CASP7,SKA2,HMMR,TUBGCP4,SKP2,BCS1L,EXOSC2,TUBB2A,ZNF260,UBE2B,PPP5C,CEP78,ZNF718,ASF1B,NCAPD2,GEMIN4,RACGAP1,MAD2L2,METTL7A,RHOT1,DNMT1
Interaction		int:DYNLL1	DYNLL1 interactions	6.88E-04	12	224	LCA5,POLH,DYRK1A,HMMR,CCDC77,RHEX,KANK1,ASF1B,DYNLL1,CLINT1,DNMT1,DCAF7
Coexpression	GeneSigDB	18757322-TableS1	Human Breast_Creighton08_2154genes	1.74E-03	29	1739	RAD51C,MRM2,NEMP1,POLR3K,TBC1D15,RNASEH2A,TBC1D5,BAG3,WDR70,APEH,HMMR,DBP,CRABP2,BCS1L,EXOSC2,TUBB2A,FARSA,KANK1,PPP5C,ASF1B,OSGEPL1,UCP2,ARID5B,NCAPD2,RACGAP1,CHST12,ALDH5A1,METTL7A,DNMT1
Coexpression	MSigDB C2: CGP Curated Gene Sets (v6.0)	M80	Genes up-regulated in TC71 and EWS502 cells (Ewing's sarcoma) by EWSR1-FLI1 [GeneID=2130;2314] as inferred from RNAi knockdown of this fusion protein.	1.74E-03	24	1276	RAD51C,MRM2,NEMP1,RNASEH2A,HACD3,BAG2,LARS,CKAP5,SKA2,HMMR,TUBGCP4,SKP2,EXOSC2,SMYD4,PPP5C,CEP78,ASF1B,TMEM245,NCAPD2,NFYA,GEMIN4,RACGAP1,POC5,DNMT1
Coexpression	MSigDB C2: CGP Curated Gene Sets (v6.0)	M10351	Genes down-regulated in T24 (bladder cancer) cells in response to the photodynamic therapy (PDT) stress.	2.94E-03	16	637	RAD51C,POLR3K,DCAF8,GATC,ERMP1,SKP2,BCS1L,DFFB,FARSA,KANK1,ADRB2,THYN1,UCP2,GEMIN4,MRPL34,ALDH5A1
Coexpression	MSigDB C2: CGP Curated Gene Sets (v6.0)	M14427	Genes down-regulated in nasopharyngeal carcinoma (NPC) compared to the normal tissue.	2.94E-03	24	1367	RAD51C,MRM2,NEMP1,NAPEPLD,RNASEH2A,HACD3,RCCD1,LARS,CKAP5,HMMR,TUBGCP4,CCDC77,SKP2,ADAM22,ZNF260,DNAJA3,CEP78,SLC25A40,OSGEPL1,GORAB,CBX1,RACGAP1,RHOT1,SCAI
Transcription Factor Binding Site		RCGCANGCGYV$NRF1 Q6	RCGCANGCGY_V$NRF1_Q6	3.11E-03	17	654	TBC1D15,RASA1,TBC1D5,POLH,DPF2,HMMR,TUBGCP4,EXOSC2,PREB,MRPL17,DNAJA3,DFFB,DPY30,NFYA,GEMIN4,MOCS2,DNMT1
Coexpression	MSigDB C7: Immunologic Signatures (v6.0)	M5300	Genes down-regulated in comparison of untreated CD4 [GeneID=920] memory T cells from old donors versus those treated with TSST at 40 h.	3.51E-03	9	200	RAD51C,POLR3K,RNASEH2A,RBM4B,CKAP5,IRF4,SNUPN,HMMR,RACGAP1
Coexpression	MSigDB C7: Immunologic Signatures (v6.0)	M8271	Genes down-regulated in B lymphocytes stimulated by anti-IgM: 3h versus 16h.	3.51E-03	9	200	EHBP1,LRRC39,NAPEPLD,RNASEH2A,DOCK8,WDR70,DROSHA,SPATA5,RHOT1
Coexpression	GeneSigDB	17952126-SuppTable2	Human Bladder_Buytaert08_651genes	3.51E-03	15	608	RAD51C,POLR3K,DCAF8,ERMP1,SKP2,BCS1L,DFFB,FARSA,KANK1,ADRB2,THYN1,UCP2,GEMIN4,MRPL34,ALDH5A1
Coexpression	GeneSigDB	18362358-Table11	Human Leukemia_Calln08_60genes	3.70E-03	5	41	RAD51C,LARS,OSGEPL1,ASXL2,RHOT1
Coexpression	MSigDB H: Hallmark Gene Sets (v6.0)	M5922	Genes up-regulated during unfolded protein response, a cellular stress response related to the endoplasmic reticulum.	3.81E-03	7	113	BAG3,EXOSC2,TUBB2A,DDX10,PREB,NFYA,GEMIN4
Coexpression	MSigDB C2: CGP Curated Gene Sets (v6.0)	M1105	Genes down-regulated in ME-A cells (breast cancer) undergoing apoptosis in response to doxorubicin [PubChem=31703].	3.81E-03	27	1781	RAD51C,TRAF6,DCAF8,RIPK1,RCCD1,HIKESHI,CKAP5,DYRK1A,DUSP19,TUBGCP4,SKP2,BCS1L,EXOSC2,ELMO1,DDX10,MRPL17,ST3GAL5,DPY30,NCAPD2,NFYA,CBX1,RACGAP1,ATP13A3,MRPL34,MAD2L2,RNF145,NEURL4

Coexpression	MSigDB C2: CGP Curated Gene Sets (v6.0)	M1463	Genes up-regulated in Caco-2 cells (intestinal epithelium) after coculture with the probiotic bacteria L. casei for 24h.	3.81E-03	14	556	NEMP1,POLR3K,ATP6V0E1,HMMR,SKP2,EXOSC2,TUBB2A,THYN1,DROSHA,GEMIN4,RACGAP1,DYNLL1,ATP13A3,DNMT1
Coexpression Atlas	FaceBase_RNAseq	Facebase_RNAseq_e8.5_Floor Plate_2500_K3	FacebaseRNAseq_e8.5_Floor Plate_top-relative-expression-ranked_2500_k-means-cluster#3	3.94E-03	17	708	ATP6V0E1,BAG3,BAG2,LARS,TMEM138,APEH,DUSP19,TYSND1,SKP2,WDR26,DNAJA3,FARSA,PPP5C,CEP78,ASF1B,NFYA,GEMIN4
Coexpression Atlas	PCBC	ratio_ECTO_vs_SC_2500_K2	ratio_induced-Ectoderm_vs_StemCell_top-relative-expression-ranked_2500_k-means-cluster#2	3.94E-03	13	419	MRM2,POLR3K,DCAF8,SPOUT1,HACD3,HIKESHI,LARS,TMEM138,TUBGCP4,THYN1,DROSHA,GEMIN4,RACGAP1
Coexpression	MSigDB C2: CGP Curated Gene Sets (v6.0)	M2368	Genes up-regulated during later stage of differentiation of Oli-Neu cells (oligodendroglial precursor) in response to PD174265 [PubChem=4709].	4.43E-03	14	570	NEMP1,CKAP5,CASP7,SKA2,HMMR,CCDC77,SKP2,THYN1,ASF1B,NCAPD2,RACGAP1,DYNLL1,DNMT1,DCAF7
Coexpression	MSigDB C2: CGP Curated Gene Sets (v6.0)	M9516	Genes constituting the BRCA2-PCC network of transcripts whose expression positively correlated (Pearson correlation coefficient, PCC >= 0.4) with that of BRCA2 [GeneID=675] across a compendium of normal tissues.	4.43E-03	12	423	RAD51C,NEMP1,RNASEH2A,CKAP5,HMMR,SKP2,EXOSC2,NCAPD2,NFYA,CBX1,CLINT1,DNMT1
Coexpression	GeneSigDB	17229949-TableS4	Human Breast_Liu07_186genes	4.43E-03	8	172	SLC38A9,LARS,DPF2,FAM160B1,GORAB,ATP13A3,METTL7A,DCAF7
Coexpression	GeneSigDB	16597596-TableS2-3	Human Leukemia_Wilson06_50genes_DifferentialClusterC	4.84E-03	5	49	GCDH,BCS1L,EXOSC2,DYNLL1,DCAF7
Coexpression	MSigDB C2: CGP Curated Gene Sets (v6.0)	M2228	Genes down-regulated in erythroid progenitor cells from fetal livers of E13.5 embryos with KLF1 [GeneID=10661] knockout compared to those from the wild type embryos.	5.38E-03	28	1972	POLR3K,RIPK1,DOCK8,HIKESHI,POLH,CASP7,EVI2A,SKA2,TUBGCP4,FAM160B1,SKP2,ELOF1,ELMO1,INIP,CCR2,UBE2B,THYN1,PPP5C,DPY30,BTK,NFYA,RACGAP1,TOR1B,RNF145,SPATA5,CRAMP1,RHOT1,DNMT1
Coexpression	GeneSigDB	18387200-Genes	Human Breast_Mutarelli08_1488genes	6.36E-03	20	1169	RAD51C,POLR3K,RNASEH2A,POLH,LARS,CKAP5,HMMR,TUBGCP4,CRABP2,SKP2,BCS1L,EXOSC2,DDX10,MRPL17,FARSA,ASF1B,NCAPD2,GEMIN4,RACGAP1,MAD2L2
Coexpression	MSigDB C2: CGP Curated Gene Sets (v6.0)	M18120	Genes down-regulated in HCT116 cells (colon cancer) by expression of MIR192 or MIR215 [GeneID=406967;406997] at 24 h.	6.36E-03	17	893	NEMP1,SLC39A1,HACD3,LARS,DYRK1A,CASP7,ERMP1,HMMR,INIP,CEP78,SLC25A40,NFYA,RACGAP1,CHST12,TOR1B,ALDH5A1,RSBN1L
Coexpression	MSigDB C2: CGP Curated Gene Sets (v6.0)	M2156	Genes up-regulated in MCF7 cells (breast cancer) at 24 h of estradiol [PubChem=5757] treatment.	6.36E-03	10	324	NEMP1,RNASEH2A,SKP2,EXOSC2,DDX10,CEP78,ASF1B,NCAPD2,RACGAP1,DNMT1
Coexpression	MSigDB C7: Immunologic Signatures (v6.0)	M3594	Genes down-regulated in comparison of CD8 T cells at 0 h versus those at 24 h after stimulation with antigen-B7-1.	6.36E-03	8	200	POLR3K,CKAP5,IRF4,ELOF1,MRPL17,CBX1,RHOT1,DNMT1
Coexpression	MSigDB C7: Immunologic Signatures (v6.0)	M4248	Genes down-regulated in comparison of CD4 [GeneID=920] T cells treated with IL4 [GeneID=3565] and anti-IL12 at 1.5 h versus those at 72 h.	6.36E-03	8	200	RAD51C,POLR3K,RCCD1,IRF2,THYN1,GRHPR,ASF1B,MAD2L2
Coexpression	MSigDB C7: Immunologic Signatures (v6.0)	M3830	Genes up-regulated in comparison of dendritic cells (DC) stimulated with poly(I:C) (TLR3 agonist) at 2 h versus DC cells stimulated with Pam3Csk4 (TLR1/2 agonist) at 2 h.	6.36E-03	8	200	RASA1,GATC,EVI2A,SKP2,DNAJA3,CHST12,SPATA5,DNMT1
Coexpression	MSigDB C7: Immunologic Signatures (v6.0)	M8103	Genes up-regulated in unstimulated IL10 [GeneID=3586] knockout macrophages versus NFKB1 and IL10 [GeneID=4790;3586] knockout macrophages stimulated by LPS.	6.36E-03	8	200	RASA1,APEH,EVI2A,SKA2,DPF2,CCDC77,RACGAP1,HSH2D
Coexpression	MSigDB C7: Immunologic Signatures (v6.0)	M5303	Genes down-regulated in comparison of untreated CD4 [GeneID=920] memory T cells from old donors versus those treated with TSST at 72 h.	6.36E-03	8	200	RAD51C,RNASEH2A,RBM4B,CKAP5,IRF4,SNUPN,HMMR,RACGAP1

Coexpression	MSigDB C7: Immunologic Signatures (v6.0)	M3326	Genes up-regulated in comparison of polysome bound (translated) mRNA versus total mRNA in dendritic cells.	6.36E-03	8	200	SPOUT1,BAG3,BCS1L,DNAJA3,GORAB,RACGAP1,ARHGEF3,CRAMP1
Coexpression	MSigDB C7: Immunologic Signatures (v6.0)	M3591	Genes down-regulated in comparison of CD8 T cells at 0 h versus those at 24 h after stimulation with IL12 .	6.36E-03	8	200	POLR3K,CKAP5,IRF4,CRABP2,ELOF1,MRPL17,NEURL4,RHOT1
Coexpression	MSigDB C7: Immunologic Signatures (v6.0)	M4298	Genes down-regulated in comparison of naive CD8 T cells versus effector CD8 IL2RA [GeneID=3559] low T cells at.	6.36E-03	8	200	RAD51C,NAPEPLD,HIKESHI,DUSP19,ERMP1,INIP,DROSHA,CHST12
Coexpression	MSigDB C7: Immunologic Signatures (v6.0)	M9922	Genes up-regulated in B lymphocytes: untreated versus anti-IgM for 6h.	6.36E-03	8	200	EHBP1,TBC1D5,CKAP5,ELMO1,SLC25A40,UCP2,RHOT1,DNMT1
Coexpression	MSigDB C7: Immunologic Signatures (v6.0)	M6925	Genes up-regulated in B lymphocytes: control versus anti IgM and CpG oligodeoxynucleotide 1826.	6.36E-03	8	200	RNASEH2A,HIKESHI,DUSP19,HMMR,ZNF260,GRHPR,CHST12,METTL7A
Coexpression	GeneSigDB	17150101-TableS1l	Human Breast_Troester06_436genes-up-DOX-ZR75-1	6.52E-03	10	329	RNASEH2A,RCCD1,CASP7,HMMR,SKP2,SLC25A40,ASF1B,NCAPD2,RACGAP1,DNMT1
Coexpression	MSigDB C2: CGP Curated Gene Sets (v6.0)	M1744	Genes with promoters bound by E2F4 [GeneID=1874] in unstimulated hybridoma cells.	6.53E-03	15	727	NEMP1,HIKESHI,SKA2,HMMR,SKP2,EXOSC2,INIP,ASF1B,DROSHA,NCAPD2,NFYA,CBX1,RACGAP1,DNMT1,DCAF7
Coexpression	MSigDB C2: CGP Curated Gene Sets (v6.0)	M1195	Genes up-regulated in hepatocellular carcinoma (HCC) compared to normal liver samples.	8.23E-03	15	744	NEMP1,SLC39A1,HACD3,TBC1D5,BAG2,ERMP1,HMMR,TYSND1,SKP2,ELMO1,ASF1B,NCAPD2,NFYA,CBX1,DCAF7
Coexpression	MSigDB C2: CGP Curated Gene Sets (v6.0)	M5611	Genes constituting the BRCA1-PCC network of transcripts whose expression positively correlated (Pearson correlation coefficient, PCC >= 0.4) with that of BRCA1 [GeneID=672] across a compendium of normal tissues.	8.23E-03	24	1651	RAD51C,NEMP1,RNASEH2A,CKAP5,CASP7,IRF2,IRF4,DAXX,HMMR,SKP2,ADAM22,KYAT1,DDX10,FARSA,BTK,UCP2,NCAPD2,GEMIN4,ATP13A3,CLINT1,ABCG2,ALDH5A1,DNMT1,DCAF7
Coexpression	GeneSigDB	19139136-TableS3	Human Prostate_John-Aryankalayil09_2212genes	8.23E-03	23	1547	NEMP1,RCCD1,ZNF460,POLH,SKA2,DUSP19,HMMR,CCDC77,CRABP2,SKP2,KYAT1,SLC25A40,ST3GAL5,PIK3C2B,ASF1B,OSGEPL1,TTLL11,GORAB,ARID5B,NCAPD2,RACGAP1,CLINT1,RNF145
Coexpression	MSigDB C2: CGP Curated Gene Sets (v6.0)	M4077	Genes identified by method 2 as coordinately down-regulated late in HMEC cells (mammary epithelium) during acinar development in vitro.	8.23E-03	9	277	RNASEH2A,HACD3,CKAP5,SKP2,BCS1L,PREB,MRPL17,DROSHA,RACGAP1
Coexpression	MSigDB C2: CGP Curated Gene Sets (v6.0)	M1915	Genes down-regulated in neural stem cells (NSC) at 60 h after cre-lox knockout of TLX (NR2E1) [GeneID=7101].	8.23E-03	9	277	RAD51C,POLR3K,HMMR,SKP2,EXOSC2,ASF1B,NCAPD2,RACGAP1,DNMT1

Supplementary Table S6. Reactome gene sets obtained using Gene Sets Enrichment Analysis showing significant modulation between patients with low and high NEAT1 expression level. NES: Normalized Enrichment Score. Pathways in bold were found significantly enriched also in GSEA analysis run in GSE2658 series.

Gene set name	Gene set size	NES	p-value	Gene List
PI3K AKT ACTIVATION	36	1.53	0.028	AKT3, PIK3CA, PHLPP1, IRS1, IRS2, CDKN1A, CHUK, NR4A1, CDKN1B, RICTOR, FOXO1, TRIB3, NTRK1, MDM2, AKT1, RHOA, CASP9, PIK3R1, FOXO4, NGF, MLST8, CREB1, BAD, PDPK1, MTOR, FOXO3, RPS6KB2, AKT2, PIK3CB, GSK3A, TSC2, MAPKAP1, AKT1S1, THEM4, PIK3R2, PTEN
AMINO ACID TRANSPORT ACROSS THE PLASMA MEMBRANE	31	1.51	0.043	SLC7A5, SLC3A1, SLC7A1, SLC6A15, SLC7A11, SLC43A2, SLC3A2, SLC6A6, SLC7A8, SLC7A10, SLC6A12, SLC38A5, SLC7A9, SLC36A2, SLC7A3, SLC6A14, SLC7A2, SLC16A10, SLC38A2, SLC7A6, SLC7A7, SLC6A19, SLC38A1, SLC38A3, SLC43A1, SLC6A18, SLC1A5, SLC36A1, SLC38A4, SLC1A4, SLC6A20
SIGNAL TRANSDUCTION BY L1	34	1.47	0.033	ITGA2B, ITGB3, ITGAV, RPS6KA2, RPS6KA6, RPS6KA4, EGFR, ITGB1, MAP2K1, RPS6KA5, RPS6KA3, FGFR1, CSNK2B, CSNK2A2, RAC1, NCAM1, CLTC, ITGA5, MAP2K2, CSNK2A1, NRP1, ITGA9, AP2A1, RPS6KA1, PAK1, AP2B1, MAPK1, MAPK3, CLTA, AP2A2, SH3GL2, AP2S1, AP2M1, L1CAM
DIABETES PATHWAYS	122	1.40	0.042	ATF3, DDIT3, DNAJB9, DIS3, GH1, GHRL, ARFGAP1, LMNA, CCL2, RAB27A, SHC1, EXOC8, ATF6, CTDSP2, DNAJC3, TSPYL2, KLF4, EXOC1, EIF2AK3, DNAJB11, MMP1, SLC30A7, ERN1, FKBP14, SERP1, KDELR3, ACADVL, LEP, STX1A, PAPPA2, EDEM1, VAMP2, IGF2, PDIA5, HDGF, SEC11C, TPP1, PLA2G7, EXOSC7, KIF5B, HERPUD1, ATF4, PCSK2, MBTPS1, IGFBP5, ZBTB17, MBTPS2, IGFBP1, EXOSC1, HSPA5, MBOAT4, GCG, SPCS1, SPCS2, SSR1, HSP90B1, SPCS3, EXOC3, SRPRB, PLG, IGF2BP3, PAPPA, EXOC2, IGFBP3, F2, NFYB, EXOSC9, KLK3, PDIA6, IGFBP6, MMP2, WIPI1, IGFBP4, EIF2S1, ADD1, IGFALS, EXOC4, EXOC5, SYVN1, ATP6V0D1, IGFBP2, EXOSC8, PCSK1, KHSRP, GOSR2, CALR, EXOSC6, DDX11, CXXC1, SEC11A, HYOU1, IGF2BP1, INS, SEC31A, GSK3A, CUL7, BCHE, PARN, CPE, YIF1A, XBP1, DCTN1, PPP2R5B, TATDN2, TLN1, ASNS, IGF2BP2, KLHDC3, MYO5A, EXOC6, EXTL3, WFS1, CTSG, SLC30A5, EXOSC4, NFYA, DCP2, EXOSC3, EXOSC2, EXOSC5, PREB, SNAP25
PROCESSIVE SYNTHESIS ON THE LAGGING STRAND	15	-1.69	0.000	FEN1, DNA2, LIG1, RPA2, POLD1, POLA1, POLD2, POLD4, POLD3, PRIM2, RPA3, POLA2, RPA1, PRIM1, PCNA
FORMATION OF INCISION COMPLEX IN GG NER	20	-1.69	0.024	GTF2H4, RAD23B, CDK7, ERCC5, XPA, ERCC4, XPC, DDB1, CCNH, ERCC3, GTF2H3, ERCC1, RPA2, ERCC2, RPA3, GTF2H1, MNAT1, DDB2, RPA1, GTF2H2
DESTABILIZATION OF MRNA BY KSRP	16	-1.63	0.020	DIS3, EXOSC7, EXOSC1, EXOSC9, AKT1, MAPK14, EXOSC8, KHSRP, EXOSC6, PARN, MAPK11, EXOSC4, DCP2, EXOSC3, EXOSC2, EXOSC5
GLOBAL GENOMIC NER GG NER	32	-1.61	0.018	GTF2H4, RFC5, RAD23B, CDK7, ERCC5, XPA, ERCC4, XPC, DDB1, CCNH, ERCC3, GTF2H3, RFC3, RFC2, ERCC1, LIG1, RPA2, ERCC2, POLD1, POLD2, POLE, POLD4, POLD3, RPA3, GTF2H1, MNAT1, RFC4, DDB2, POLE2, RPA1, PCNA, GTF2H2
HOMOLOGOUS RECOMBINATION REPAIR OF REPLICATION INDEPENDENT DOUBLE STRAND BREAKS	16	-1.60	0.020	BRCA2, TP53BP1, MDC1, RAD50, RAD51, LIG1, NBN, RPA2, ATM, H2AFX, RAD52, MRE11A, RPA3, RPA1, BRCA1, BRIP1
RESOLUTION OF AP SITES VIA THE MULTIPLE NUCLEOTIDE PATCH REPLACEMENT PATHWAY	17	-1.57	0.042	MPG, TDG, MBD4, FEN1, NTHL1, CCNO, POLB, MUTYH, APEX1, LIG1, POLD1, POLD2, OGG1, POLD4, POLD3, SMUG1, PCNA
METABOLISM OF NUCLEOTIDES	69	-1.57	0.010	AK5, PNP, ADSS, NT5E, UPB1, GUK1, NT5C2, UPP1, NT5C1B, NT5C1A, TXN, GLRX, AMPD1, UCK2, ADSSL1, TK2, AMPD2, CMPK1, ADK, HPRT1, GSR, IMPDH1, DPYD, UPP2, DCTD, UMPS, AMPD3, GDA, APRT, PFAS, TXNRD1, AK1, DUT, NT5C, AGXT2, ADAL, GMPR, DGUOK, ADSL, GMPS, UCK1, GMPR2, TYMP, CAT, NT5M, RRM1, DPYS, NME1, IMPDH2, ADA, AK2, ATIC, XDH, NME4, CTPS2, DHODH, PPAT, GART, CDA, RRM2B, TK1, PAICS, GPX1, TYMS, DTYMK, DCK, NME2, CAD, RRM2
BASE EXCISION REPAIR	19	-1.56	0.047	MPG, TDG, MBD4, LIG3, FEN1, NTHL1, CCNO, XRCC1, POLB, MUTYH, APEX1, LIG1, POLD1, POLD2, OGG1, POLD4, POLD3, SMUG1, PCNA

NUCLEOTIDE EXCISION REPAIR	48	-1.56	0.044	GTF2H4, TCEA1, RFC5, RAD23B, POLR2A, CDK7, ERCC5, XPA, POLR2B, POLR2D, ERCC4, XAB2, XPC, DDB1, CCNH, POLR2J, POLR2F, ERCC3, POLR2L, POLR2C, POLR2G, GTF2H3, ERCC8, POLR2I, POLR2K, RFC3, RFC2, ERCC6, ERCC1, LIG1, RPA2, ERCC2, POLD1, POLD2, POLE, POLD4, POLD3, POLR2H, POLR2E, RPA3, GTF2H1, MNAT1, RFC4, DDB2, POLE2, RPA1, PCNA, GTF2H2
KINESINS	24	-1.54	0.034	KIF3B, KLC1, KIF5B, KIFAP3, KIF26A, KIF2B, KIF9, KIF2A, KIF4B, KLC3, KLC2, KIF4A, KLC4, KIF22, KIF3C, KIF5A, KIFC1, KIF2C, KIF18A, KIF11, KIF20A, KIF23, RACGAP1, KIF15
EXTENSION OF TELOMERES	27	-1.52	0.040	RFC5, FEN1, DNA2, TERT, NHP2, DKC1, RFC3, RFC2, WRAP53, LIG1, RPA2, POLD1, POLA1, POLD2, POLE, POLD4, POLD3, PRIM2, RPA3, RUVBL2, POLA2, RUVBL1, RFC4, POLE2, RPA1, PRIM1, PCNA
ACTIVATION OF THE PRE REPLICATIVE COMPLEX	30	-1.51	0.033	RPA4, CDK2, CDC45, DBF4, MCM4, ORC1, CDT1, ORC5, ORC6, RPA2, ORC3, ORC4, POLA1, POLE, MCM5, CDC7, PRIM2, MCM10, MCM6, RPA3, CDC6, POLA2, MCM2, MCM7, ORC2, MCM8, POLE2, MCM3, RPA1, PRIM1
LAGGING STRAND SYNTHESIS	19	-1.51	0.047	RFC5, FEN1, DNA2, RFC3, RFC2, LIG1, RPA2, POLD1, POLA1, POLD2, POLD4, POLD3, PRIM2, RPA3, POLA2, RFC4, RPA1, PRIM1, PCNA
SYNTHESIS AND INTERCONVERSION OF NUCLEOTIDE DI AND TRIPHOSPHATES	17	-1.51	0.025	AK5, GUK1, TXN, GLRX, CMPK1, GSR, TXNRD1, AK1, RRM1, NME1, AK2, NME4, CTPS2, RRM2B, DTYMK, NME2, RRM2
NUCLEOTIDE LIKE PURINERGIC RECEPTORS	16	-1.48	0.043	GPR17, LPAR4, P2RY11, ADORA2A, P2RY1, P2RY12, P2RY4, LPAR6, ADORA3, ADORA1, P2RY6, P2RY14, ADORA2B, P2RY10, P2RY2, P2RY13
FACTORS INVOLVED IN MEGAKARYOCYTE DEVELOPMENT AND PLATELET PRODUCTION	117	-1.46	0.042	HDAC2, MAFK, IRF1, HIST1H3H, GATA3, MFN1, CDC42, EHD1, IFNA16, RAD51B, RAB5A, IFNA21, H3F3B, DOCK1, KIF3B, EP300, MAFG, SIN3A, DOCK6, PRKAR2B, ZFPM2, KLC1, KIF5B, KIFAP3, IFNA5, IFNA10, JMJD1C, MAFF, GATA2, RAC1, MFN2, CAPZA2, IFNB1, CAPZA1, ZFPM1, KIF26A, KIF2B, KIF9, KDM1A, PRKACB, IFNA4, KIF2A, PRKAR1B, DOCK9, AKAP10, WEE1, CABLES2, PRKACG, GATA5, CDK2, IFNA14, EHD2, H3F3A, GATA1, CREBBP, KIF4B, DOCK2, SH2B1, KLC3, ITPK1, IFNA8, GATA6, IFNA2, AK3, IRF7, IFNA6, KLC2, DOCK5, SH2B3, HBG2, GATA4, IFNA7, PRKAR2A, HBE1, PRKACA, VPS45, SH2B2, IFNA17, HBB, NFE2, JAK2, PRKAR1A, KIF4A, KLC4, IRF3, RCOR1, HMG20B, HBD, KIF22, CBX5, ABL1, KIF3C, HDAC1, KIF5A, DOCK3, CDK5, DOCK8, HIST1H3B, CABLES1, KIFC1, KIF2C, MYB, IRF2, AKAP1, HIST1H3E, HIST1H3G, DOCK4, KIF18A, TP53, RAD51C, HIST1H3I, KIF11, KIF20A, KIF23, DOCK10, RACGAP1, KIF15
DARPP 32 EVENTS	24	-1.45	0.043	PPP2CB, PRKAR2B, PPP3CA, PPP2CA, PDE4C, PPP3R1, PDE4B, PRKACB, PDE4D, PRKAR1B, CALM1, PRKACG, CALM2, PPP2R1A, PRKAR2A, PRKACA, PPP1CA, PRKAR1A, CALM3, PPP3CB, PPP1R1B, PPP2R1B, CDK5, PPP2R5D
CYCLIN A B1 ASSOCIATED EVENTS DURING G2 M TRANSITION	15	-1.39	0.048	CDK7, CDC25B, CCNH, WEE1, PKMYT1, CCNA1, XPO1, MNAT1, CDC25C, CDC25A, CCNA2, PLK1, CCNB1, CCNB2, CDK1

Supplementary Table S7 lncRNAs significantly under- and overexpressed in NEAT1 quartile IV versus I.

lncRNA	ID	CHR.	Score(d)	Fold Change
NEAT1	ENSG00000245532	11q13	9.48	1.78
RP11-439L18.1	ENSG00000232618	6q24	6.89	4.49
MTUS2-AS1	ENSG00000179141	13q12	4.51	2.05
NARF-IT1	ENSG00000266236	17q25	4.47	2.24
AC116366.5	ENSG00000238160	5q31	4.19	1.41
RP11-574F21.2	ENSG00000228606	1q32	4.14	2.77
MIR22HG	ENSG00000186594	17p13	4.11	2.83
RP1-90J20.8	ENSG00000224846	6p25	4.10	2.04
RP11-215P8.3	ENSG00000248559	5q31	3.99	1.88
RP4-605O3.4	ENSG00000272368	12q13	3.96	1.73
AC133644.2	ENSG00000280721	2p11	3.76	3.22
RP11-169E6.1	ENSG00000261173	16q11	3.74	1.61
C3orf35	ENSG00000198590	3p22	3.73	1.71
TTLL7-IT1	ENSG00000233061	1p31	3.69	2.63
RP11-638I2.8	ENSG00000258666	14q32	3.68	1.90
RP11-421L21.2	ENSG00000235795	1p21	3.60	2.15
C22orf24	ENSG00000128254	22q12	3.53	2.14
RP1-45I4.3	ENSG00000227192	6q24	3.52	1.85
MIR29A	ENSG00000226380	7q32	3.52	2.19
LINC01481	ENSG00000257815	12q15	3.49	1.85
WI2-85898F10.1	ENSG00000235091	22q13	3.46	3.46
RP11-253L19.3	ENSG00000255670	12p13	3.45	1.92
AC127904.2	ENSG00000230732	3q29	3.40	1.95
RP11-646J21.2	ENSG00000255133	11p13	3.32	1.41
RP11-203J24.8	ENSG00000227218	9q34	3.31	2.94
LINC01619	ENSG00000257242	12q21	3.29	3.87
CTB-131B5.5	ENSG00000254363	5q31	3.29	1.57
RP11-3D4.3	ENSG00000259408	15q14	3.25	1.40
RORA-AS1	ENSG00000245534	15q22	-4.57	0.55
DDX11-AS1	ENSG00000245614	12p11	-4.22	0.50

Supplementary Table S8. Molecular and clinical characteristics of 55 MM patients.

Sample Features	**N/%**
Patients	**55**
Median age at diagnosis	**67**
Bone damage	**60%**
Median BM-PC infiltrate	**50%**
del(13)	**53%**
del(17)	**7%**
t(4;14)	**13%**
t(11;14)	**20%**
MAF-trx	**7%**
HD	**31%**
1q gain	**49%**
1p loss	**11%**
International Staging System (ISS)	
stage I	**19**
stage II	**19**
stage III	**17**
R-ISS	
stage I	**12**
stage II	**34**
stage III	**9**
Median overall survival (OS)	**52 months**
Median time to next treatment (TNT)	**23 months**
***globaltest* OS**	***p*-value**
PRIMER 5'	0.903
PRIMER 3'	0.977
***globaltest* TNT**	***p*-value**
PRIMER 5'	0.655
PRIMER 3'	0.933